Available online at www.sciencedirect.com
SCIENCE DIRECT
Physica D 214 (2006) 101–119
PHYSICA D
www.elsevier.com/locate/physd

Multistability and stable asynchronous periodic oscillations in a multiple-delayed neural system

S.A. Campbell[a,b,*], I. Ncube[a], J. Wu[c]

[a] Department of Applied Mathematics, University of Waterloo, Waterloo, ON N2L 3G1, Canada
[b] Centre for Nonlinear Dynamics in Physiology and Medicine, McGill University, Montréal, QC H3G 1Y6, Canada
[c] Department of Mathematics and Statistics, York University, Toronto, ON M3J 1P3, Canada

Received 13 July 2005; accepted 22 December 2005
Available online 30 January 2006
Communicated by C.K.R.T. Jones

Abstract

We consider a network of three identical neurons with multiple discrete signal transmission delays. The model for such a network is a system of nonlinear delay differential equations. After some consideration of the absolute synchronization of the system and the global attractivity of the zero solution, we present a detailed discussion about the boundaries of the stability region of the trivial solution. This allows us to determine the possible codimension one bifurcations which occur in the system. In particular, we show the existence of standard Hopf bifurcations giving rise to synchronized periodic solutions and of D_3 equivariant Hopf bifurcations giving rise to three types of periodic solutions: phase-locked, mirror-reflecting, and standing waves. Hopf–Hopf and Hopf–steady state bifurcations interactions are shown to exist and give rise to coexistence of stable synchronized and desynchronized solutions. Perturbation techniques coupled with the Floquet theory are used to determine the stability of the phase-locked oscillations.

Keywords: Neural networks; Delay differential equations; Phase-locked solutions; Floquet theory; Stability; Multistability

1. Introduction

In this paper we study a network of three identical neurons in which there are distinct, discrete time delays in the signal transmission of self connection and the nearest-neighbour interaction. This network is shown schematically in Fig. 1.1, and modelled by the system of nonlinear delay differential equations

$$\dot{u}_j(t) = -\mu u_j(t) + AF(u_j(t-T_s)) + B[G(u_{j-1}(t-T_n)) + G(u_{j+1}(t-T_n))], \qquad (1.1)$$

with $j \mod 3$; where T_s and T_n are, respectively, the signal transmission delays for self- and nearest-neighbour connections. Throughout this paper, we use activation functions $F, G : \mathbb{R} \to \mathbb{R}$ satisfying the following assumptions:

1. $F(0) = G(0) = 0$, $F'(0) = G'(0) = \gamma > 0$, $F'(x)$, $G'(x) > 0$ for all $x \in \mathbb{R}$;
2. $xF''(x), xG''(x) < 0$ for all $x \neq 0$;
3. $-\infty < \lim_{x\to\pm\infty} F(x), G(x) < \infty$;
4. F, G are C^3 smooth and $F'''(0), G'''(0) < 0$.

A special case, which will be used in some parts of our work here, is

$$F(x) = G(x) = \tanh(\gamma x)$$

with some $\gamma > 0$.

Note that (1.1) has D_3 symmetry since the vector field is invariant under permutation of the coordinates, i.e. the transformation $(u_1, u_2, u_3) \to (u_2, u_3, u_1)$ and under the reflection $(u_1, u_2, u_3) \to (u_1, u_3, u_2)$ and its permutations. The symmetries of the equation lead to various invariant subspaces for the semiflow of the delay differential equation (DDE). The permutation leads to the invariant line $u_1 = u_2 = u_3$, and the reflections to the invariant planes $u_j = u_{j+1}$, $j \mod 3$.

* Corresponding author at: Department of Applied Mathematics, University of Waterloo, Waterloo, ON N2L 3G1, Canada.
E-mail addresses: sacampbell@uwaterloo.ca (S.A. Campbell), incube@math.uwaterloo.ca (I. Ncube).

0167-2789/$ - see front matter © 2006 Elsevier B.V. All rights reserved.
doi:10.1016/j.physd.2005.12.008

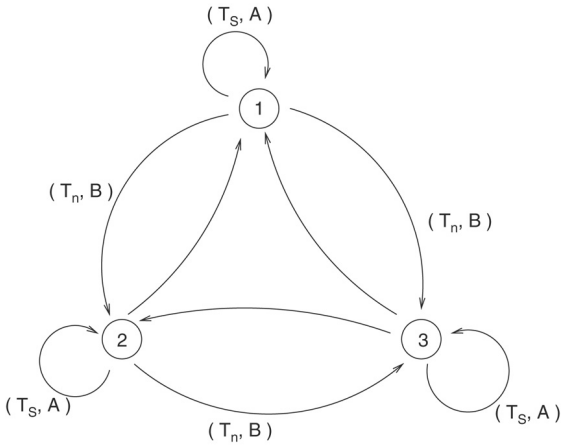

Fig. 1.1. Architecture of a network of three identical neurons with multiple time delays. The parameters T_s and T_n denote, respectively, the self-connection and nearest-neighbour connection signal transmission delays, while A and B are, respectively, the synaptic strengths of self- and nearest-neighbour connections.

We shall rescale (1.1), using the following change of variables: $\tilde{u}_j = \gamma u_j$, $\tilde{t} = \mu t$. Introducing the parameters $\alpha = \frac{\gamma}{\mu}A$, $\beta = \frac{\gamma}{\mu}B$, $\tau_s = \mu T_s$, $\tau = \mu T_n$, Eq. (1.1) then becomes

$$\dot{u}_j(t) = -u_j(t) + \alpha f(u_j(t-\tau_s)) + \beta[g(u_{j-1}(t-\tau)) + g(u_{j+1}(t-\tau))], \tag{1.2}$$

where j mod 3, $f(x) = F(\frac{x}{\gamma})$, $g(x) = G(\frac{x}{\gamma})$ and we have dropped the tildes on t and u_j for notational clarity. Note that f, g satisfy assumptions 1–4 above, with $f'(0) = g'(0) = 1$.

Let $h = \max\{\tau, \tau_s\}$ and denote by $\mathcal{C}$ the Banach space of continuous mappings from $[-h, 0]$ to $\mathbb{R}^3$ equipped with the usual super-norm. $\mathcal{C}$ is the standard phase space of the semiflow defined by Eq. (1.2), and our goal is to describe the global dynamics of the model equation (1.2) that depicts the computational performance of the network under consideration.

Following the definitions of [53], we say that a solution of (1.2) is *asymptotically synchronous* if the ω-limit set of the solution is contained in the set of *synchronous phase points* given by

$$\{\boldsymbol{\phi} = (\phi_1, \phi_2, \phi_3)^{\mathrm{T}} \in \mathcal{C} : \phi_1 = \phi_2 = \phi_3\},$$

and we say that system (1.2) is *absolutely synchronous* if every solution of (1.2) is asymptotically synchronous for all fixed nonnegative values of τ_s and τ. As will be shown (in Section 2), if $|\alpha| + |\beta| < 1$, then (1.2) is absolutely synchronous. If, in addition, $|\alpha| + 2|\beta| < 1$, then every solution of (1.2) is convergent to zero as $t \to \infty$ regardless of the size of the delays τ_s and τ.

This suggests that symmetric bifurcation theory should provide a very natural way to investigate the global dynamics of (1.2). Namely, we start with the case of small $|\alpha|$ and $|\beta|$, and then gradually increase these two synaptic weights and vary the two time lags, in order to see how the dynamical behaviours of system (1.2) change through the interchange of stability and mode interaction of different solutions bifurcated from the trivial solution. As will be shown, due to the structure of the characteristic equation of the linearization of system (1.2) at the trivial solution, single/double root pitchfork/Hopf bifurcations can occur. Further, various types of Hopf–Hopf, Hopf–steady state interactions will be shown to occur. Such points can lead to very interesting dynamics such as multistability and quasiperiodicity [4,9,10,22,49]. The double root bifurcations arise due to the symmetry of the system and thus well-known results from the literature of symmetric bifurcation theory (see, for example, [19,30,51]), are used to show that the Hopf bifurcations can give rise to four types of periodic solutions, namely: synchronized, phase-locked, mirror-reflecting, and standing waves. The stability of these periodic solutions is clearly important in applications, but also poses significant computational challenges. In this and subsequent work, we hope to show that the single model (1.2) can generate each of the aforementioned stable oscillation patterns by varying the four parameters $(\alpha, \beta, \tau_s, \tau)$. It should be mentioned that the stable spatial-temporal patterns alluded to above have been reported through different (usually PDE) models, but to the best of our knowledge, there is no single model that exhibits all of these stable patterns through variation of the parameters.

The current paper will establish

1. concrete criteria for the absolute synchronization of model (1.2) and global attractivity of the trivial solution;
2. a detailed description of the stability boundaries of the trivial solution;
3. the existence of mode interactions indicated by the intersection of the aforementioned stability boundaries;
4. the stability of the bifurcated phase-locked oscillations.

The issues of absolute synchronization of model (1.2) and global attractivity of the trivial solution will be addressed in Section 2, with the help of a Liapunov functional. We then, using a method adapted from previous work [4,47,48], present a detailed analysis of various boundaries of the stability region for the trivial solution in Section 3. The main focus here is on the asymptotic analysis of the boundaries as the four parameters approach certain limits suggested by our criterion of the global attractivity of the zero solution in Section 2. In Section 4 we discuss the bifurcations which occur in the system and how these may be used to determine when the system will synchronize/desynchronize. We also determine the various possible interactions of the stability boundaries that lead to mode interaction, multistability and exchange of the stability of bifurcated spatio-temporal patterns.

Finally, in Sections 5 and 6, we concentrate on the stability of the bifurcated phase-locked periodic solutions resulting from the double root single Hopf bifurcation. To this end, we employ standard perturbation theory to approximate such oscillations, followed by an application of Floquet theory to determine the stability. More precisely, our approach is based on the analytic construction of an approximation to the bifurcating phase-locked oscillation using a perturbation procedure together with an application of the Fredholm alternative theory for functional differential equations. Once this approximation is constructed, we then use the Poincaré–Lindstedt series expansion to compute the Floquet exponents of the bifurcating phase-locked oscillation, assisted by the symbolic computation language

MAPLE. This allows us to depict a smooth surface in a certain parameter space which determines the stability/criticality of the phase-locked oscillation. In an on-going project, we are extending our approach to address the stability of standing waves and mirror-reflecting waves.

One of the seminal articles on the perturbation approach we propose to employ in the current paper is that of Gopalsamy and Leung [21], in which a system of two neurons with a single discrete delay is studied. It was shown that such a system is capable of generating and sustaining temporal periodic behaviour. In addition, the stability of an approximation to the periodic oscillation is determined through a combination of standard perturbation and Floquet theories, and the perturbation argument is crucial in constructing an approximation to the periodic solution.

It has been widely observed and reported (see [2–6,8,38] and references therein) that a coupled system of multiple-delayed differential equations exhibits some fascinating bifurcation phenomena as linear stability is lost. By far the most popular approach that has been used to perform such studies has been centre manifold and normal form theory, partly because of the obvious elegance of the theory. In practice, however, the computations involved in the determination of the centre manifold, and hence normal form, may be quite cumbersome, thereby rendering efforts in that direction an exercise in futility. This is especially true for coupled systems of three or more multiple-delayed neurons. To the best of our knowledge, there is currently no sufficiently robust symbolic computation language which is capable of handling such calculations. We are interested in symbolic, as opposed to numerical, computations primarily because the systems that we study are characterized by multiple parameters and we would like to characterize stability in the most general terms possible; not just for specific parameter values. Such a generality is essential for our longterm goal to exhibit all possible stable spatio-temporal patterns through a single delay differential equation system by varying the parameters.

Despite the symbolic computation difficulties mentioned above, some interesting and insightful work has been done over the years. For example, in [4], a scalar multiple-delayed differential equation of the form

$$\dot{u}(t) = f_1(u(t - T_1)) + f_2(u(t - T_2)),$$

where $f_j(x) = -A_j \tanh(x)$, $j = 1, 2$ ($A_j \in \mathbb{R}^+$), is considered. The bifurcations occurring as linear stability is lost are studied via the construction of a centre manifold. In particular, the nature of Hopf and more degenerate, higher codimension bifurcations are explicitly determined. We note that the linear stability analysis of this equation was also studied in [26,31,48]. Attention should also be drawn to the earlier work of Nussbaum [37] for a scalar delay differential equation with negative feedback and multiple delays, where an ejective fixed point theorem is used to obtain the existence of periodic solutions for a wide range of parameters. Further interesting studies may also be found in [11,13–17,47,41–45,50,52] for networks of two and four neurons, and the excellent monograph [35] for the justification of studying small networks of neurons with delayed feedback.

We note also the work of Orosz and Stépán [39], who studied a quite general system with translational symmetry and one time delay using centre manifold and normal form analysis. They applied their results to a two dimensional car following model with periodic boundary conditions, which leads to a system with a ring structure and uni-directional coupling. Orosz et al. [40] studied the n dimensional version of this model using local bifurcation theory and numerical continuation analysis.

In [53], Wu et al. studied the model equation (1.2) when the two delays τ_s and τ are identical, and it was shown that, in a certain region of the space (α, β), each solution of the network is convergent to the set of synchronous states in the space. Furthermore, it was shown that this synchronization is independent of the size of the delay. Also, a *bifurcation surface* was obtained, as the graph of a continuous function of $\tau = \tau(\alpha, \beta)$ in some region of (α, β), where Hopf bifurcation of periodic solutions occurs. This work was based on symmetric Hopf bifurcation theory in [51] and the normal form theory for DDEs developed in [18], and it was possible to depict the bifurcation surface and to describe the stability of phase-locked periodic solutions since the calculation of the normal form up to the 5th order was still feasible as only one time delay is involved. In the case where there are two distinct delays, the symbolic calculation of the normal form, even up to the third order in the case of single Hopf bifurcation of (synchronized) periodic solutions, is a formidable challenge, as shown in [36]. This motivates us to use singular perturbation techniques as an alternative approach.

2. Synchronization and global stability

Recall that a solution of (1.2) is *asymptotically synchronous* if the ω-limit set of the solution is contained in the set of *synchronous phase points* given by

$$\{\boldsymbol{\phi} = (\phi_1, \phi_2, \phi_3)^{\mathrm{T}} \in \mathcal{C} : \phi_1 = \phi_2 = \phi_3\}.$$

System (1.2) is *absolutely synchronous* if every solution of (1.2) is asymptotically synchronous for all fixed nonnegative values of τ_s and τ.

Theorem 1. *If* $|\alpha| + |\beta| < 1$, *then* (1.2) *is absolutely synchronous.*

Proof. Let $\tau_s, \tau \geq 0$ be fixed and define $h = \max\{\tau_s, \tau\}$. Consider a given solution $u : [-h, \infty) \to \mathbb{R}^3$ of (1.2) and let $y(t) = u_1(t) - u_2(t)$. Then from (1.2) we find, for all $t \geq 0$,

$$\begin{aligned}\dot{y}(t) &= -y(t) + \alpha[f(u_1(t - \tau_s)) - f(u_2(t - \tau))] \\ &\quad - \beta[g(u_1(t - \tau)) - g(u_2(t - \tau))] \\ &= -y(t) + \alpha p(t) y(t - \tau_s) - \beta q(t) y(t - \tau),\end{aligned}$$

where

$$p(t) = \int_0^1 f'(v u_1(t - \tau_s) + (1 - v) u_2(t - \tau_s))\, \mathrm{d}v$$

$$q(t) = \int_0^1 g'(v u_1(t - \tau) + (1 - v) u_2(t - \tau))\, \mathrm{d}v.$$

Due to the C^1-smoothness of f, g, the boundedness of $u_1, u_2 : [-h, \infty) \to \mathbb{R}$, and the normalization and concavity conditions on f and g, we can find $p^*, q^* \in (0, 1]$ such that $p(t) \le p^*$ and $q(t) \le q^*$ for all $t \ge 0$.

Let

$$V(t) = y^2(t) + |\alpha| p^* \int_{t-\tau_s}^{t} y^2(\theta)\,\mathrm{d}\theta + |\beta| q^* \int_{t-\tau}^{t} y^2(\theta)\,\mathrm{d}\theta, \quad t \ge 0.$$

Then

$$\begin{aligned}\frac{\mathrm{d}}{\mathrm{d}t}V(t) &= 2y(t)[-y(t) + \alpha p(t) y(t-\tau_s) - \beta q(t) y(t-\tau)] \\ &\quad + |\alpha| p^* [y^2(t) - y^2(t-\tau_s)] \\ &\quad + |\beta| p^* [y^2(t) - y^2(t-\tau)] \\ &\le -2y^2(t) + |\alpha| p^* [y^2(t) + y^2(t-\tau_s)] \\ &\quad + |\beta| q^* [y^2(t) + y^2(t-\tau)] \\ &\quad + |\alpha| p^* [y^2(t) - y^2(t-\tau_s)] \\ &\quad + |\beta| p^* [y^2(t) - y^2(t-\tau)] \\ &\le -2(1 - |\alpha| - |\beta|) y^2(t),\end{aligned}$$

from which it follows that

$$\begin{aligned}&y^2(t) + |\alpha| p^* \int_{t-\tau_s}^{t} y^2(\theta)\,\mathrm{d}\theta + |\beta| q^* \int_{t-\tau}^{t} y^2(\theta)\,\mathrm{d}\theta \\ &\quad + 2(1 - |\alpha| - |\beta|) \int_0^t y^2(\theta)\,\mathrm{d}\theta \\ &\le y^2(0) + |\alpha| p^* \int_{-\tau_s}^{0} y^2(\theta)\,\mathrm{d}\theta + |\beta| q^* \int_{-\tau}^{0} y^2(\theta)\,\mathrm{d}\theta.\end{aligned}$$

Consequently, $\int_0^\infty y^2(\theta)\,\mathrm{d}\theta < \infty$.

Note that y is bounded on $[-\tau, \infty)$, and thus $\dot{y}$ is bounded on $[0, \infty)$. This, together with $y \in L^2([0, \infty))$, implies (by a theorem of Barbălat [1,20]) that $\lim_{t\to\infty} y(t) = 0$. Therefore, $\lim_{t\to\infty}[u_1(t) - u_2(t)] = 0$. Similarly, we can show that

$$\lim_{t\to\infty}[u_2(t) - u_3(t)] = \lim_{t\to\infty}[u_3(t) - u_1(t)] = 0. \quad \square$$

We conjecture that all solutions will be asymptotically synchronous for parameter values such that no asynchronous periodic solution or steady state bifurcates from the trivial solution. A more precise statement of the conjecture will be formulated in Section 3.

In the following, we are going to show that, by imposing more constraints on α and β, we are able to obtain a global attractivity result for the trivial solution. To state the result, let us note that a solution which is asymptotically synchronous will satisfy

$$\lim_{t\to\infty} |u_j(t) - u(t)| = 0, \quad j = 1, 2, 3,$$

where $u(t)$ is a solution of the scalar DDE

$$\dot{u}(t) = -u(t) + \alpha f(u(t-\tau_s)) + 2\beta g(u(t-\tau)). \tag{2.1}$$

Theorem 2. *If $|\alpha| + 2|\beta| < 1$, then every solution of (1.2) converges to zero as $t \to \infty$.*

Proof. Note that $|\alpha| + |\beta| \le |\alpha| + 2|\beta|$, so by Theorem 1 all solutions are asymptotically synchronous. To prove the theorem, we will only need to show that every given solution $u(t)$ of (2.1) converges to zero as $t \to \infty$.

Note that we can rewrite (2.1) as

$$\dot{u}(t) = -u(t) + \alpha p(t) u(t-\tau_s) + 2\beta q(t) u(t-\tau)$$

with

$$p(t) = \int_0^1 f'(vu(t-\tau_s))\,\mathrm{d}v, \quad q(t) = \int_0^1 g'(vu(t-\tau))\,\mathrm{d}v.$$

From the conditions assumed on f and g there exist $p^*, q^* \in (0, 1]$ such that $p(t) \le p^*$ and $q(t) \le q^*$.

Let

$$V(t) = u^2(t) + |\alpha| p^* \int_{t-\tau_s}^{t} u^2(s)\,\mathrm{d}s + 2|\beta| q^* \int_{t-\tau}^{t} u^2(s)\,\mathrm{d}s$$

and use the same technique as that for Theorem 1, we can show that $u(t) \to 0$ as $t \to \infty$. $\square$

Remark. We note that the above result can also be obtained by using a Liapunov function coupled with the Razumikhin technique. Let $V(u) = \max_{1\le i\le 3} |u_i|$ and note that the upper-right Dini derivative of $V(u(t))$ then satisfies $D^+V(u(t)) \le -V(u(t)) + (|\alpha| + 2|\beta|) \max_{s\in[-h,0]} V(u(t+s))$ and hence $D^+V(u(t)) \le -(1 - |\alpha| - 2|\beta|)V(u(t)) < 0$ if $\max_{s\in[-h,0]} V(u(t+s)) \le V(u(t)) \ne 0$. This enables us to apply the Haddock–Terjeki's LaSalle invariance principle [23] of Razumikhin type to conclude that every solution of (1.2) converges to zero as $t \to \infty$. This idea was previously used by Bélair [3] for a scalar DDE with a single delay.

3. Linear stability analysis

The previous section determined parameter values for which the solutions of system (1.2) approach any synchronized solution, and, in particular, the simplest synchronized solution, the trivial solution, $u_1 = u_2 = u_3 = 0$. One way to study the approach of solutions to other synchronized and nonsynchronized solutions is through the analysis of bifurcations from the trivial solution. To this end, this section gives a detailed analysis of the linearized stability of the trivial solution of (1.2). This is followed, in Section 4, by a discussion of the bifurcations which occur when stability is lost and how these indicate when synchronization can and cannot occur. Much of our work in this section is adapted from that of Shayer and Campbell [47], who studied a model which was essentially a nonsymmetric version of (1.2) with two neurons instead of three, and that of Bélair and Campbell [4] who studied the corresponding scalar equation. The work of this section will culminate in a representation of the stability region of the trivial solution of (1.2) in the parameter space consisting of one of the delays and one of the gains. This approach has also been used by Stépán [48] to study DDE's with multiple delays.

We begin by linearizing (1.2) about the trivial solution $u_1 = u_2 = u_3 = 0$, yielding

$$\begin{aligned}\dot{u}_i(t) &= -u_i(t) + \alpha u_i(t-\tau_s) + \beta u_{i-1}(t-\tau) \\ &\quad + \beta u_{i+1}(t-\tau).\end{aligned} \tag{3.1}$$

This leads to the characteristic equation

$$\Delta_1^2(\lambda)\Delta_2(\lambda) \stackrel{def}{=} (\lambda + 1 - \alpha e^{-\lambda\tau_s} + \beta e^{-\lambda\tau})^2 \times (\lambda + 1 - \alpha e^{-\lambda\tau_s} - 2\beta e^{-\lambda\tau}) = 0. \quad (3.2)$$

It follows from standard results [25,27,29,48] that the trivial solution of (1.2) will be locally asymptotically stable if all the roots of the characteristic equation (3.2) have negative real parts and unstable if at least one root has positive real part. We will thus establish results about the local asymptotic stability of the trivial solution of (1.2) by analyzing the roots of (3.2).

In particular, in the next subsection, we describe some subsets of the parameter space where we can prove directly that all roots of (3.2) have negative real parts. In Section 3.2 we describe the curves in the (β, τ) plane where stability may be lost, i.e. the curves where the characteristic equation (3.2) has roots with zero real parts. This is followed by an examination of how the geometry of these curves changes as the parameters α and τ_s are varied. Finally, in Section 3.3, the results are put together to give a complete description of the region in $(\alpha, \beta, \tau_s, \tau)$ parameter space where the trivial solution is locally asymptotically stable.

3.1. Subsets of the stability region

To begin, we give two delay-independent results.

Theorem 3. *If the parameters satisfy $|\beta| < \frac{1}{2}(1 - |\alpha|)$ the trivial solution of (1.2) is locally asymptotically stable for all $\tau_s \geq 0$ and $\tau \geq 0$.*

Proof. This result follows from the global stability result of Theorem 2. It can also be proven by direct analysis of the characteristic equation in a manner similar to that of [47, Theorem 1]. □

Remark. It can also be shown in a manner similar to that of [47, Theorem 1] that the trivial solution is locally asymptotically stable for $\beta = 0$, $\alpha = -1$, $\tau_s \geq 0$ and $\tau \geq 0$.

Theorem 4. *If the parameters satisfy $\alpha < -1$, $|\beta| < -\frac{\alpha}{2}$, $0 \leq \tau_s < -\frac{1}{2\alpha}$ and $\tau \geq 0$, then all the roots of the characteristic equation (3.2) have negative real part.*

Proof. To begin, let $\lambda = \nu + i\omega$ in the second factor of (3.2). Separating into real and imaginary parts, we obtain

$$\nu = -1 + \alpha e^{-\nu\tau_s}\cos(\omega\tau_s) + 2\beta e^{-\nu\tau}\cos(\omega\tau) \quad (3.3)$$

and

$$\omega = -\alpha e^{-\nu\tau_s}\sin(\omega\tau_s) - 2\beta e^{-\nu\tau}\sin(\omega\tau). \quad (3.4)$$

We now assume that (3.3) and (3.4) have roots ν and ω, where $\omega \geq 0$ (without loss of generality since complex roots of (3.2) come in complex conjugate pairs). From (3.4), if $\nu \geq 0$ and using the conditions imposed on β, we find that $\omega < -2\alpha$. The condition $0 \leq \tau_s < -\frac{1}{2\alpha}$ then implies that $0 \leq \omega\tau_s < 1$. Hence, $1/2 < \cos(1) < \cos(\omega\tau_s) \leq 1$ and $0 \leq \sin(\omega\tau_s) < \sin(1) < 1$.

Isolating the last term in both (3.3) and (3.4), squaring and adding, we obtain the necessary condition

$$(\nu+1)^2 + \omega^2 - 2\alpha e^{-\nu\tau_s}\{(\nu+1)\cos(\omega\tau_s) - \omega\sin(\omega\tau_s)\} + \alpha^2 e^{-2\nu\tau_s} - 4\beta^2 e^{-2\nu\tau} = 0, \quad (3.5)$$

for a solution of (3.3) and (3.4) to exist. For fixed values of ω, τ_s, and τ, we call the left-hand side of (3.5) $M(\nu)$ and note that

$$M(0) = 1 - 2\alpha\cos(\omega\tau_s) + \alpha^2 + \omega^2 + 2\alpha\omega\sin(\omega\tau_s) - 4\beta^2.$$

Since $\sin(\omega\tau_s) < \omega\tau_s$ and $\tau_s < -\frac{1}{2\alpha}$, then

$$\omega^2 + 2\alpha\omega\sin(\omega\tau_s) \geq \omega^2(1 + 2\alpha\tau_s) > 0,$$

which, recalling that $\alpha < 0$, $\cos(\omega\tau_s) > 0$ and $4\beta^2 < \alpha^2$, yields $M(0) > 0$. Taking the derivative of $M(\nu)$ with respect to ν, we obtain

$$\frac{dM}{d\nu} = 2\Big\{4\tau\beta^2 e^{-2\nu\tau} - \alpha\omega\tau_s e^{-\nu\tau_s}\sin(\omega\tau_s) + (\nu+1)\left[1 + \alpha\tau_s e^{-\nu\tau_s}\cos(\omega\tau_s)\right] - \alpha e^{-\nu\tau_s}\left[\cos(\omega\tau_s) + \alpha\tau_s e^{-\nu\tau_s}\right]\Big\}. \quad (3.6)$$

Since $\alpha < 0$, $\omega \geq 0$, $\tau_s \geq 0$, $\tau \geq 0$, $\nu \geq 0$ and $\sin(\omega\tau_s) \geq 0$, the first two terms in the first line of expression (3.6) are nonnegative. We now consider the other two in turn.

(1) From $0 \leq \tau_s < -\frac{1}{2\alpha}$ and $\nu \geq 0$, we have $0 < e^{-\nu\tau_s} \leq 1$. Combining this with $\cos(\omega\tau_s) \leq 1$, we obtain

$$(\nu+1)\left[1 + \alpha\tau_s e^{-\nu\tau_s}\cos(\omega\tau_s)\right] \geq (\nu+1)\left(1 - \frac{1}{2}\right) > 0.$$

(2) From $\alpha < 0$, $\frac{1}{2} < \cos(1) < \cos(\omega\tau_s)$, $\tau_s < -\frac{1}{2\alpha}$, and $0 < e^{-\nu\tau_s} \leq 1$,

$$-\alpha e^{-\nu\tau_s}\left[\cos(\omega\tau_s) + \alpha\tau_s e^{-\nu\tau_s}\right] > -\alpha e^{-\nu\tau_s}\left(\cos(1) - \frac{1}{2}\right) > 0.$$

Thus, $\frac{dM}{d\nu} > 0$ for $\nu \geq 0$. Since $M(0) > 0$, we conclude that $M(\nu) > 0$ if $\nu \geq 0$. Thus if $M(\nu) = 0$, then $\nu < 0$; i.e., all roots of $\Delta_2(\lambda)$ have negative real part. It may be shown in a similar manner that all the roots of $\Delta_1(\lambda)$ have negative real part. □

The following theorem shows that parameter values analogous to those of Theorem 4, but with $\alpha > 0$, do not lie inside the region of stability, i.e., the trivial solution is unstable for these parameter values.

Theorem 5. *If $\alpha > 1$, then the trivial solution of (1.2) is unstable for all values of β, $\tau_s \geq 0$ and $\tau \geq 0$. If $\alpha = 1$, then the trivial solution of (1.2) is unstable for all values of $\beta \neq 0$, $\tau_s \geq 0$ and $\tau \geq 0$.*

Proof. Recall from the characteristic equation (3.2) that $\Delta_1(\lambda) = (\lambda + 1 - \alpha e^{-\lambda\tau_s} + \beta e^{-\lambda\tau})$. Then, with $\alpha > 1$ and $\beta \leq 0$,

$$\Delta_1(0) = (1 - \alpha + \beta) < 0$$

and, for $\lambda \in \mathbb{R}$,

$$\lim_{\lambda\to+\infty}\Delta_1(\lambda) = \lim_{\lambda\to+\infty}[\lambda + 1 - \alpha e^{-\lambda\tau_s} + \beta e^{-\lambda\tau}] = +\infty$$

for all $\beta \leq 0$, $\tau_s \geq 0$ and $\tau \geq 0$. Hence, as $\Delta_1 : \mathbb{R} \to \mathbb{R}$ is a continuous function, there exists a $\lambda^* > 0$ such that $\Delta_1(\lambda^*) = 0$ for any fixed values of $\tau_s \geq 0$, $\tau \geq 0$, $\beta \leq 0$ and $\alpha > 1$.

Now consider $\Delta_2(\lambda) = (\lambda + 1 - \alpha e^{-\lambda\tau_s} - 2\beta e^{-\lambda\tau})$. For $\beta \geq 0$, with $\alpha > 1$

$$\Delta_2(0) = 1 - \alpha - 2\beta < 0$$

and, for $\lambda \in \mathbb{R}$,

$$\lim_{\lambda\to+\infty} \Delta_2(\lambda) = \lim_{\lambda\to+\infty} [\lambda + 1 - \alpha e^{-\lambda\tau_s} - 2\beta e^{-\lambda\tau}] = +\infty.$$

Hence, as $\Delta_2 : \mathbb{R} \to \mathbb{R}$ is a continuous function, there exists a $\lambda^* > 0$ such that $\Delta_2(\lambda^*) = 0$ for any fixed values of $\tau_s \geq 0$, $\tau \geq 0$, $\beta \geq 0$ and $\alpha > 1$.

When $\alpha = 1$, similar arguments show that $\Delta_1(\lambda)$ has a positive real root for any fixed values of $\tau_s \geq 0$, $\tau \geq 0$ and $\beta < 0$, and that $\Delta_2(\lambda)$ has a positive real root for any fixed values of $\tau_s \geq 0$, $\tau \geq 0$ and $\beta > 0$.

Thus, the characteristic equation has a positive real root for all β and all $\tau_s \geq 0$, $\tau \geq 0$ when $\alpha > 1$ and for all $\beta \neq 0$ and all $\tau_s \geq 0$, $\tau \geq 0$ when $\alpha = 1$. Hence the trivial solution is unstable for these parameter values. □

3.2. Curves of characteristic roots with zero real part

As the parameters are varied, stability may be lost by a real root of the characteristic equation passing through zero, or by a pair of complex conjugate roots passing through the imaginary axis. The former occurs when $\beta = \frac{1}{2}(1 - \alpha)$, where the characteristic equation has a simple zero root, and when $\beta = \alpha - 1$, where the characteristic equation has a double zero root. The latter occurs as described below.

The characteristic equation has a simple pair of pure imaginary roots $\lambda = \pm i\omega$ for parameter values such that $\Delta_2(\pm i\omega) = 0$. This occurs when $\alpha, \beta, \tau_s, \tau, \omega$ satisfy

$$\begin{aligned} 1 - \alpha\cos\omega\tau_s &= 2\beta\cos\omega\tau \\ \omega + \alpha\sin\omega\tau_s &= -2\beta\sin\omega\tau. \end{aligned} \tag{3.7}$$

For fixed α and τ_s this occurs along the curves (β_H^+, τ_{Hk}^+) and (β_H^-, τ_{Hk}^-) where

$$\beta_H^\pm = \pm\frac{1}{2}\sqrt{1 + \alpha^2 + \omega^2 + 2\alpha\omega\sin\omega\tau_s - 2\alpha\cos\omega\tau_s}, \tag{3.8}$$

$$\begin{aligned} \tau_{Hk}^+ &= \frac{1}{\omega}\mathrm{Arctan}\left[\frac{-\omega - \alpha\sin\omega\tau_s}{1 - \alpha\cos(\omega\tau_s)}\right] \\ &\quad + \begin{cases} 2k\pi/\omega, & 1 - \alpha\cos\omega\tau_s < 0 \\ (2k+1)\pi/\omega, & 1 - \alpha\cos\omega\tau_s > 0, \end{cases} \end{aligned} \tag{3.9}$$

$$\begin{aligned} \tau_{Hk}^- &= \frac{1}{\omega}\mathrm{Arctan}\left[\frac{-\omega - \alpha\sin\omega\tau_s}{1 - \alpha\cos(\omega\tau_s)}\right] \\ &\quad + \begin{cases} 2k\pi/\omega, & 1 - \alpha\cos\omega\tau_s < 0 \\ (2k+1)\pi/\omega, & 1 - \alpha\cos\omega\tau_s > 0. \end{cases} \end{aligned} \tag{3.10}$$

The characteristic equation has a repeated pair of pure imaginary roots $\lambda = \pm i\omega$ for parameter values such that $\Delta_1(\pm i\omega) = 0$. This occurs when $\alpha, \beta, \tau_s, \tau, \omega$ satisfy

$$\begin{aligned} 1 - \alpha\cos\omega\tau_s &= -\beta\cos\omega\tau, \\ \omega + \alpha\sin\omega\tau_s &= \beta\sin\omega\tau. \end{aligned} \tag{3.11}$$

For fixed α and τ_s this occurs along the curves $(\beta_{Hd}^+, \tau_{Hdk}^+)$ and $(\beta_{Hd}^-, \tau_{Hdk}^-)$ where

$$\begin{aligned} \beta_{Hd}^\pm &= \pm\sqrt{1 + \alpha^2 + \omega^2 + 2\alpha\omega\sin\omega\tau_s - 2\alpha\cos\omega\tau_s} \\ &= 2\beta_H^\pm, \end{aligned} \tag{3.12}$$

$$\begin{aligned} \tau_{Hdk}^+ &= \frac{1}{\omega}\mathrm{Arctan}\left[\frac{-\omega - \alpha\sin\omega\tau_s}{1 - \alpha\cos(\omega\tau_s)}\right] \\ &\quad + \begin{cases} 2k\pi/\omega, & 1 - \alpha\cos\omega\tau_s < 0 \\ (2k+1)\pi/\omega, & 1 - \alpha\cos\omega\tau_s > 0, \end{cases} \end{aligned} \tag{3.13}$$

$$\begin{aligned} \tau_{Hdk}^- &= \frac{1}{\omega}\mathrm{Arctan}\left[\frac{-\omega - \alpha\sin\omega\tau_s}{1 - \alpha\cos(\omega\tau_s)}\right] \\ &\quad + \begin{cases} 2k\pi/\omega, & 1 - \alpha\cos\omega\tau_s > 0 \\ (2k+1)\pi/\omega, & 1 - \alpha\cos\omega\tau_s < 0. \end{cases} \end{aligned} \tag{3.14}$$

For fixed α and τ_s Eqs. (3.8)–(3.10) and (3.12)–(3.14) define families of curves in the β, τ plane, parametrized by ω. In order to describe how these curves form the boundary of the stability region, we first state some limits.

$$\begin{aligned} &\lim_{\omega\to0} \beta_H^\pm = \pm\frac{|1-\alpha|}{2}, \\ &\lim_{\omega\to0} \tau_{Hk}^\pm = \begin{cases} \dfrac{1 + \alpha\tau_s}{\alpha - 1}, & k = 0, \mp(\alpha - 1) > 0 \\ \infty, & \text{otherwise} \end{cases} \end{aligned} \tag{3.15}$$

$$\begin{aligned} &\lim_{\omega\to0} \beta_{Hd}^\pm = \pm|1 - \alpha|, \\ &\lim_{\omega\to0} \tau_{Hdk}^\pm = \begin{cases} \dfrac{1 + \alpha\tau_s}{\alpha - 1}, & k = 0, \pm(\alpha - 1) > 0 \\ \infty, & \text{otherwise} \end{cases} \end{aligned} \tag{3.16}$$

$$\begin{aligned} &\lim_{\omega\to\infty} \beta_H^\pm = \pm\infty, \quad \lim_{\omega\to\infty} \tau_{Hk}^\pm = 0, \\ &\lim_{\omega\to\infty} \beta_{Hd}^\pm = \pm\infty, \quad \lim_{\omega\to\infty} \tau_{Hdk}^\pm = 0. \end{aligned} \tag{3.17}$$

Consider the case when $|\alpha| < 1$. Then

$$\lim_{\omega\to\infty} \mathrm{Arctan}\left[\frac{-\omega - \alpha\sin\omega\tau_s}{1 - \alpha\cos(\omega\tau_s)}\right] = -\frac{\pi}{2}$$

and the curves have the following asymptotic behaviour as $\omega \to \infty$

$$\begin{aligned} &\beta_H^\pm \sim \pm\frac{\omega}{2}, \quad \tau_{Hk}^+ \sim \left[-\frac{\pi}{2} + 2k\pi\right]\Big/\omega, \\ &\tau_{Hk}^- \sim \left[-\frac{\pi}{2} + (2k+1)\pi\right]\Big/\omega, \end{aligned} \tag{3.18}$$

$$\begin{aligned} &\beta_{Hd}^\pm \sim \pm\omega, \quad \tau_{Hdk}^+ \sim \left[-\frac{\pi}{2} + (2k+1)\pi\right]\Big/\omega, \\ &\tau_{Hdk}^- \sim \left[-\frac{\pi}{2} + 2k\pi\right]\Big/\omega. \end{aligned} \tag{3.19}$$

This implies the following asymptotic behaviour as $\beta \to \infty$

$$\tau_{Hk}^+ \sim \frac{(4k-1)\pi}{4\beta} = -\frac{\pi}{4\beta}, \frac{3\pi}{4\beta}, \frac{7\pi}{4\beta}, \ldots \tag{3.20}$$

$$\tau_{Hdk}^+ \sim \frac{(4k+1)\pi}{2\beta} = \frac{\pi}{2\beta}, \frac{5\pi}{2\beta}, \frac{9\pi}{2\beta}, \ldots \tag{3.21}$$

and as $\beta \to -\infty$

$$\tau^-_{Hk} \sim -\frac{(4k+1)\pi}{4\beta} = -\frac{\pi}{4\beta}, -\frac{5\pi}{4\beta}, -\frac{9\pi}{4\beta}, \dots \tag{3.22}$$

$$\tau^-_{Hdk} \sim -\frac{(4k-1)\pi}{2\beta} = \frac{\pi}{2\beta}, -\frac{3\pi}{2\beta}, -\frac{7\pi}{2\beta}, \dots \tag{3.23}$$

We now give some lemmas about how the geometry of the curves described above changes as α and τ_s are varied.

Lemma 1. *If $|\alpha| \le 1$, then*

1. *the curves (β^+_H, τ^+_{Hk}) are bounded on the left by the line $\beta = \frac{1-|\alpha|}{2}$;*
2. *the curves (β^-_H, τ^-_{Hk}) are bounded on the right by the line $\beta = \frac{|\alpha|-1}{2}$;*
3. *the curves $(\beta^+_{Hd}, \tau^+_{Hdk})$ are bounded on the left by the line $\beta = 1 - |\alpha|$;*
4. *the curves $(\beta^-_{Hd}, \tau^-_{Hdk})$ are bounded on the right by the line $\beta = |\alpha| - 1$.*

Proof. From Eq. (3.7), which holds along $\beta = \beta^+_H$, we have

$$\beta^+_H \ge \beta^+_H \cos(\omega\tau^+_{Hk}) = \frac{1-\alpha\cos(\omega\tau_s)}{2} \ge \frac{1-|\alpha|}{2},$$

which establishes result 1. Since $\beta^-_H = -\beta^+_H$, this also establishes result 2. Results 3 and 4 can be shown in an analogous manner. □

Lemma 2. *The curves of pure imaginary eigenvalues have the property that β^+_H and β^+_{Hd} are monotone increasing functions of ω, β^-_H and β^-_{Hd} are monotone decreasing functions of ω and satisfy $\beta^+_H > \frac{1}{2}|1-\alpha|$, $\beta^-_H < -\frac{1}{2}|1-\alpha|$, $\beta^+_{Hd} > |1-\alpha|$, $\beta^-_{Hd} < -|1-\alpha|$, for all $\omega > 0$ if τ_s satisfies*

$$0 \le \tau_s \le -1 + \sqrt{1 + \frac{1}{|\alpha|}}.$$

When $\alpha < 0$, the converse is also true.

Proof. Consider first β^+_H. Differentiating (3.8) with respect to ω, we obtain

$$\frac{\mathrm{d}\beta^+_H}{\mathrm{d}\omega} = \frac{1}{4\beta^+_H}[\omega + \alpha(1+\tau_s)\sin(\omega\tau_s) + \alpha\omega\tau_s\cos(\omega\tau_s)]. \tag{3.24}$$

For $\tau_s = 0$ and $\omega > 0$, $\frac{\mathrm{d}\beta^+_H}{\mathrm{d}\omega} = \frac{\omega}{4\beta^+_H} > 0$. For $\omega\tau_s > 0$, $\alpha\cos(\omega\tau_s) \ge -|\alpha|$ and $\alpha\sin(\omega\tau_s) > -|\alpha|\omega\tau_s$, hence

$$\begin{aligned}\frac{\mathrm{d}\beta^+_H}{\mathrm{d}\omega} &> \frac{\omega}{4\beta^+_H}(1 - 2|\alpha|\tau_s - |\alpha|\tau_s^2)\\ &= \frac{\omega|\alpha|}{4\beta^+_H}\left[\frac{1}{|\alpha|} + 1 - (\tau_s+1)^2\right]\\ &\ge 0\end{aligned}$$

for $\tau_s \le -1 + \sqrt{1+|\alpha|}$. It now follows from the first limit in (3.15) that $\beta^+_H > \frac{1}{2}|1-\alpha|$ for all $\omega > 0$.

To prove the converse, consider the Taylor expansion of $\frac{\mathrm{d}\beta^+_H}{\mathrm{d}\omega}$ about $\omega = 0$:

$$\begin{aligned}\frac{\mathrm{d}\beta^+_H}{\mathrm{d}\omega} &= \omega\left\{\frac{1+2\alpha\tau_s+\alpha\tau_s^2}{|1-\alpha|}\right\}\\ &\quad - \frac{1}{2|1-\alpha|}\omega^3\left\{\frac{\alpha\tau_s^3}{3}(4+\tau_s) + \frac{(1+\alpha\tau_s+\alpha\tau_s^2)^2}{(1-\alpha)^2}\right\}\\ &\quad + O(\omega^5).\end{aligned}$$

If $\tau_s > -1 + \sqrt{1+\frac{1}{|\alpha|}}$ and $\alpha < 0$, then the first term of this expression is negative, and hence $\beta^+_H(\omega)$ is decreasing for ω sufficiently close to zero.

The proofs for β^-_H and $\beta^\pm_{Hd}$ follow in a similar manner. □

Remark. We denote the special value $\tau_s = -1 + \sqrt{1+\frac{1}{|\alpha|}}$ by its equivalent form

$$\tau_s^{(1)} = \frac{1}{\left(1+\sqrt{1+\frac{1}{|\alpha|}}\right)|\alpha|}, \quad \alpha \in \mathbb{R} \tag{3.25}$$

and refer to it as the *first transition point*.

From the previous discussion, it is clear that for $\tau_s < \tau_s^{(1)}$, the minimum (maximum) values of β^+_H, β^+_{Hd} (β^-_H, β^-_{Hd}) occur when $\omega = 0$. For $\tau_s > \tau_s^{(1)}$ this is not necessarily the case. Let $\omega_{\min}$ be the smallest positive value of ω such that $\frac{\mathrm{d}\beta^+_{Hd}}{\mathrm{d}\omega} = 0$, and define $\beta^{\min}_{Hd} = \beta^+_{Hd}(\omega_{\min})$. Then for $\tau_s > \tau_s^{(1)}$, $\beta^{\min}_{Hd}$ is the minimum value of β^+_{Hd} and $-\beta^{\min}_{Hd}$ is the maximum value of β^-_{Hd}.

Another important transition will occur when this minimum value of β^+_{Hd} crosses the line $\beta = \frac{1}{2}(1-\alpha)$. We therefore define the *second transition point* to be the value $\tau_s^{(2)}$ such that when $\tau_s = \tau_s^{(2)}$, $\beta^{\min}_{Hd} = \frac{1}{2}(1-\alpha)$. Note that $\tau_s^{(2)}$ is defined implicitly by

$$\begin{aligned}&1 + \alpha^2 + \omega^2_{\min} + 2\alpha\omega_{\min}\sin(\omega_{\min}\tau_s^{(2)}) - 2\alpha\cos(\omega_{\min}\tau_s^{(2)})\\ &\quad = \frac{1}{4}(1-\alpha)^2,\end{aligned} \tag{3.26}$$

where $\omega_{\min}$ is the smallest root of

$$\begin{aligned}&\omega_{\min} + \alpha(1+\tau_s^{(2)})\sin(\omega_{\min}\tau_s^{(2)})\\ &\quad + \alpha\omega_{\min}\tau_s^{(2)}\cos(\omega_{\min}\tau_s^{(2)}) = 0.\end{aligned} \tag{3.27}$$

Lemma 3. *The second transition occurs only if $\alpha > 1$ or if $\alpha < -\frac{1}{3}$.*

Proof. Recall from Lemma 1 that if $|\alpha| \le 1$ then $\beta^{\min}_{Hd} > 1 - |\alpha|$. Thus this transition will occur for $|\alpha| \le 1$ only if $1 - |\alpha| < \frac{1}{2}(1-\alpha)$. When $0 \le \alpha \le 1$, $1 - |\alpha| = 1 - \alpha \ge \frac{1}{2}(1-\alpha)$, so the transition never occurs. When $-1 \le \alpha < 0$, $1 - |\alpha| = 1 + \alpha < \frac{1}{2}(1-\alpha)$ if $\alpha < -\frac{1}{3}$.

From Lemma 4 below, $\beta^{\min}_{Hd} \ge 0$ if $|\alpha| > 1$. We thus conclude that the second transition always occurs if $\alpha > 1$ or $\alpha < -1$. The result follows. □

A third transition corresponds to when the curves $(\beta_H^{\pm}, \tau_{Hk}^{\pm})$ and $(\beta_{Hd}^{\pm}, \tau_{Hdk}^{\pm})$ touch the τ axis. The following lemma determines when this occurs.

Lemma 4. *Let α be fixed. If $|\alpha| < 1$, then $\beta_H(\omega), \beta_{Hd}(\omega) \neq 0$ for any $\tau_s \geq 0$ and any $\omega \in (0, \infty)$. If $|\alpha| > 1$, then there exist countably many values of τ_s for which $\beta_H(\omega) = \beta_{Hd}(\omega) = 0$ for some $\omega \in (0, \infty)$.*

Proof. We begin by letting $\beta = 0$ in Eqs. (3.7) (or, equivalently, (3.11)) and assume that $\omega > 0$. This results in

$$\alpha \cos(\omega\tau_s) = 1 \quad \text{and} \quad \alpha \sin(\omega\tau_s) = -\omega. \tag{3.28}$$

Clearly, these equations can only be satisfied, for positive ω, if $1 < |\alpha|$. In this case, squaring and adding (3.28) produces

$$\omega = \sqrt{\alpha^2 - 1}. \tag{3.29}$$

Substituting this expression into the first equation of (3.28) and solving for τ_s, we obtain:

$$\tau_s = \begin{cases} \dfrac{1}{\sqrt{\alpha^2-1}}\left[\text{Arccos}\left(\dfrac{1}{\alpha}\right) + 2n\pi\right] & \text{if } \alpha < -1 \\ \dfrac{1}{\sqrt{\alpha^2-1}}\left[-\text{Arccos}\left(\dfrac{1}{\alpha}\right) + (2n+2)\pi\right] & \text{if } \alpha > 1, \end{cases} \tag{3.30}$$

where Arccos is the principal branch of the inverse cosine function which has the range $[0, \pi]$. □

Remark. We are particularly interested in the smallest positive value of τ_s for which the curves touch the τ axis. Since the trivial solution is unstable if $\alpha > 1$ we focus on the case $\alpha < -1$, denote the corresponding value of τ_s by

$$\tau_s^{(3)} = \frac{1}{\sqrt{\alpha^2-1}}\left\{\text{Arccos}\left(\frac{1}{\alpha}\right)\right\}, \quad \alpha < -1, \tag{3.31}$$

and refer to it as the *third transition point*.

One final transition is associated with the finite limit in (3.15) and (3.16). Define

$$\tau^* \stackrel{def}{=} \frac{1+\alpha\tau_s}{\alpha - 1}, \quad \tau_s^* \stackrel{def}{=} -\frac{1}{\alpha}, \tag{3.32}$$

and note that $\tau^* > 0$ if $\alpha > 1$ and $\tau_s \geq 0$ and $\tau^* \geq 0$ if $\alpha < 0$ and $\tau_s \geq \tau_s^*$. Thus this transition occurs when α passes through 1 or when τ_s passes through τ_s^* with $\alpha < 0$. The transition corresponds to the appearance of a new member of the family of curves of pure imaginary eigenvalues, which has a finite limit as $\omega \to 0$.

Lemma 5. *For $0 \leq \alpha < 1$ only the first transition occurs. For $\alpha < 0$, the transition points, when they exist, are ordered as follows*

$$\tau_s^{(1)} < \tau_s^{(2)} < \tau_2^{(3)}$$

and

$$\tau_s^{(1)} < \tau_s^* < \tau_2^{(3)}.$$

Proof. Let $\alpha < 0$. Since $\beta_{Hd}^{\min} = \beta_{Hd}(0) = 1 - \alpha > \frac{1}{2}(1-\alpha)$ for $\tau_s \leq \tau_s^{(1)}$, we must have $\tau_s^{(1)} < \tau_s^{(2)}$. Since $\frac{1}{2}(1-\alpha) > 0$ and $\tau_s^{(3)}$ corresponds to the first value of τ_s for which $\beta_{Hd}^{\min} = 0$, we must have $\tau_s^{(2)} < \tau_s^{(3)}$.

The ordering of $\tau_s^{(1)}$ and τ_s^* is easily seen from Eqs. (3.25) and (3.32). Now consider, for $\alpha < -1$,

$$\tau_s^{(3)} - \tau_s^* = -\frac{1}{\alpha}\left[\frac{1}{\sqrt{1-\frac{1}{\alpha^2}}}\text{Arccos}\left(\frac{1}{\alpha}\right) - 1\right].$$

Simple analysis shows that the quantity in [ ] is always positive, hence $\tau_s^* < \tau_s^{(3)}$. □

Remark. The transition point $\tau_s^{(2)}$ is difficult to study analytically. However, numerical results indicate that there exists $\alpha^* < -1$ such that $\tau_s^* < \tau^{(2)}$ for $\alpha^* < \alpha < -1/3$ and $\tau^{(2)} < \tau_s^*$ for $\alpha < \alpha^*$.

3.3. Full stability region

We will now describe the full stability region of the trivial solution in the β, τ plane, as α and τ_s are varied. Recall that Theorem 3 indicates that the trivial solution is stable in the vertical strip $|\beta| < \frac{1}{2}(1 - |\alpha|), \tau \geq 0$ for $|\alpha| < 1$ and all nonnegative values of τ_s. Further, Theorem 4 indicates that it is stable in the vertical strip $|\beta| < -\frac{\alpha}{2}, \tau \geq 0$ for $\alpha < -1$ and τ_s nonnegative and sufficiently small. The full region of stability is found from these subsets by increasing/decreasing β until the first curve where the characteristic equation (3.2) has a root with zero real part is reached. Using the analysis of the geometry of these curves given in the previous subsection, we can describe the full region of local asymptotic stability, as given below.

1. $\alpha > 1$: There is no stability region, cf. Theorem 5.
2. $\alpha = 1$: The trivial solution is unstable if $\beta \neq 0$. If $\beta = 0$ the stability is not determined by the linearization.
3. $0 \leq \alpha < 1$: (See Fig. 3.1)
   (a) $0 \leq \tau_s < \tau_s^{(1)}$. The stability region is bounded on the right by the line $\beta = \frac{1-\alpha}{2}$ and on the left by the line $\beta = \alpha - 1$ and the curve (β_H^-, τ_{H0}^-), i.e. it is given by the union of the following regions
   $$\alpha - 1 < \beta < \frac{1-\alpha}{2}, \quad 0 \leq \tau \leq \tau^{int};$$
   $$\frac{\alpha-1}{2} < \beta < \frac{1-\alpha}{2}, \quad \tau \geq \tau^{int};$$
   $$\beta_H^- < \beta < \frac{\alpha-1}{2}, \quad \tau^{int} \leq \tau < \tau_{H0}^-,$$
   where $\tau^{int} = \tau_{H0}^-(\omega^{int})$ and ω^{int} is such that $\beta_H^-(\omega^{int}) = \alpha - 1$.
   (b) $\tau_s > \tau_s^{(1)}$. Applying Lemma 1 shows that the boundary on the right is still the line $\beta = \frac{1-\alpha}{2}$ and that the boundary on the left is now made up of various pieces of the line $\beta = \alpha - 1$ and the curves $(\beta_H^-, \tau_{Hk}^-), k \geq 0$.
4. $-1/3 \leq \alpha < 0$:

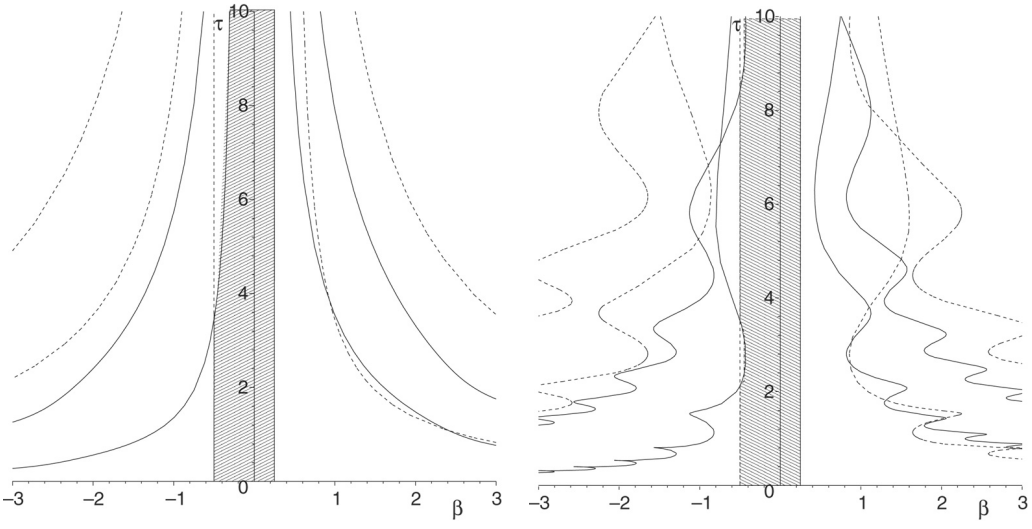

(a) $0 \le \tau_s < \tau_s^{(1)}$. (b) $\tau_s^{(1)} \le \tau_s$.

Fig. 3.1. Region of stability of the trivial solution for $0 \le \alpha < 1$. Solid (dashed) curves correspond to parameter values where $\Delta_2(\lambda)$ ($\Delta_1(\lambda)$) has a pair of pure imaginary roots. Solid (dashed) vertical lines correspond to parameter values where $\Delta_2(\lambda)$ ($\Delta_1(\lambda)$) has a zero root. Actual parameter values: $\alpha = 0.5$, $\tau_s = 0.7, 6.0$.

(a) $0 \le \tau_s < \tau_s^{(1)}$. Same as case 3(a). The stability region is bounded on the right by the line $\beta = \frac{(1-\alpha)}{2}$ and on the left by the line $\beta = \alpha - 1$ and the curve (β_H^-, τ_{H0}^-), i.e. it is given by the union of the following regions

$$\alpha - 1 < \beta < \frac{(1-\alpha)}{2}, \quad 0 \le \tau \le \tau^{int};$$

$$\frac{(\alpha-1)}{2} < \beta < \frac{(1-\alpha)}{2}, \quad \tau \ge \tau^{int};$$

$$\beta_H^- < \beta < \frac{(\alpha-1)}{2}, \quad \tau^{int} \le \tau < \tau_{H0}^-,$$

where $\tau^{int} = \tau_{H0}^-(\omega^{int})$ and ω^{int} is such that $\beta_H^-(\omega^{int}) = \alpha - 1$.

(b) $\tau_s^{(1)} < \tau_s < \tau_s^*$. The right boundary is made up of pieces of the line $\beta = \frac{1-\alpha}{2}$ and pieces of the curves (β_H^+, τ_{Hk}^+), $k > 0$, and the left boundary by pieces of the line $\beta = \alpha - 1$ and pieces of the curves (β_H^-, τ_{Hk}^-), $k \ge 0$.

(c) $\tau_s > \tau_s^*$. The right boundary is made up of pieces of the line $\beta = \frac{1-\alpha}{2}$ and pieces of the curves (β_H^+, τ_{Hk}^+), $k \ge 0$, and the left boundary by pieces of the line $\beta = \alpha - 1$ and pieces of the curves (β_H^-, τ_{Hk}^-), $k \ge 0$ and of the curve $(\beta_{Hd}^-, \tau_{Hd0}^-)$.

5. $-1 \le \alpha < -1/3$:

(a) $0 \le \tau_s < \tau_s^{(1)}$. Same as case 3(a).

(b) $\tau_s^{(1)} \le \tau_s < \tau_s^*$. Same as case 4(b).

(c) $\tau_s^* < \tau_s < \tau_s^{(2)}$. Same as case 4(c).

(d) $\tau_s > \tau_s^{(2)}$. Same as case (c), except that the right boundary may also contain pieces of the curves $(\beta_{Hd}^+, \tau_{Hdk}^+)$, $k \ge 0$ and the left boundary may also contain pieces of the curves $(\beta_{Hd}^-, \tau_{Hdk}^-)$, $k \ge 0$.

6. $\alpha < -1$: (See Fig. 3.2)

(a) $0 \le \tau_s < \tau_s^{(1)}$. Same as case 3(a).

(b) $\tau_s^{(1)} \le \tau_s < \tau_s^*$. Same as case 4(b).

(c) $\tau_s^* < \tau_s < \tau_s^{(2)}$. Same as case 4(c).

(c′) $\tau_s^{(2)} < \tau_s < \tau_s^*$. The right boundary is made up of pieces of the line $\beta = \frac{1-\alpha}{2}$ and pieces of the curves (β_H^+, τ_{Hk}^+), $k > 0$ and $(\beta_{Hd}^+, \tau_{Hkd}^+)$, $k \ge 0$, and the left boundary by pieces of the line $\beta = \alpha - 1$ and pieces of the curves (β_H^-, τ_{Hk}^-), $k \ge 0$ and $(\beta_{Hd}^-, \tau_{Hdk}^-)$, $k > 0$.

(d) $\max(\tau_s^{(2)}, \tau_s^*) < \tau_s < \tau_s^{(3)}$. Same as case 5(d).

(e) $\tau_s > \tau_s^{(3)}$. There is no longer a stability region.

We close this section by noting that the stability regions described in this section bear a striking similarity of structure to those obtained by [4] for a scalar system with two delays and by [48] for a two dimensional system with two delays.

4. Bifurcation, desynchronization and multistability

In the previous section, we determined all points in parameter space where the characteristic equation (3.2) has roots with zero real parts, i.e., where the trivial solution of (1.2) has eigenvalues with zero real parts. Varying one or more parameters in the system (1.2) so as to pass through such a point may cause a *bifurcation*, i.e., a qualitative change in the type of solutions admitted by the DDE. Such points are important, particularly when they lie on the boundary of the stability region of the trivial solution, as they determine the observable behaviour of the system.

We begin this section with a study of the bifurcations which occur in (1.2) when a single parameter is varied. For this system, there are four such codimension one bifurcations: a standard steady state bifurcation, which can occur when the factor $\Delta_2(\lambda)$ of the characteristic equation (3.2) has a single zero root; an equivariant steady state bifurcation, which can occur when $\Delta_1(\lambda)$ has a single zero root; a standard Hopf bifurcation, which can occur when $\Delta_2(\lambda)$ has a pair of pure imaginary eigenvalues; and an equivariant Hopf bifurcation which can occur when $\Delta_2(\lambda)$ has a pair of pure imaginary roots. It is straightforward to check that the conditions for the various bifurcations are satisfied when, say, β is taken to be the

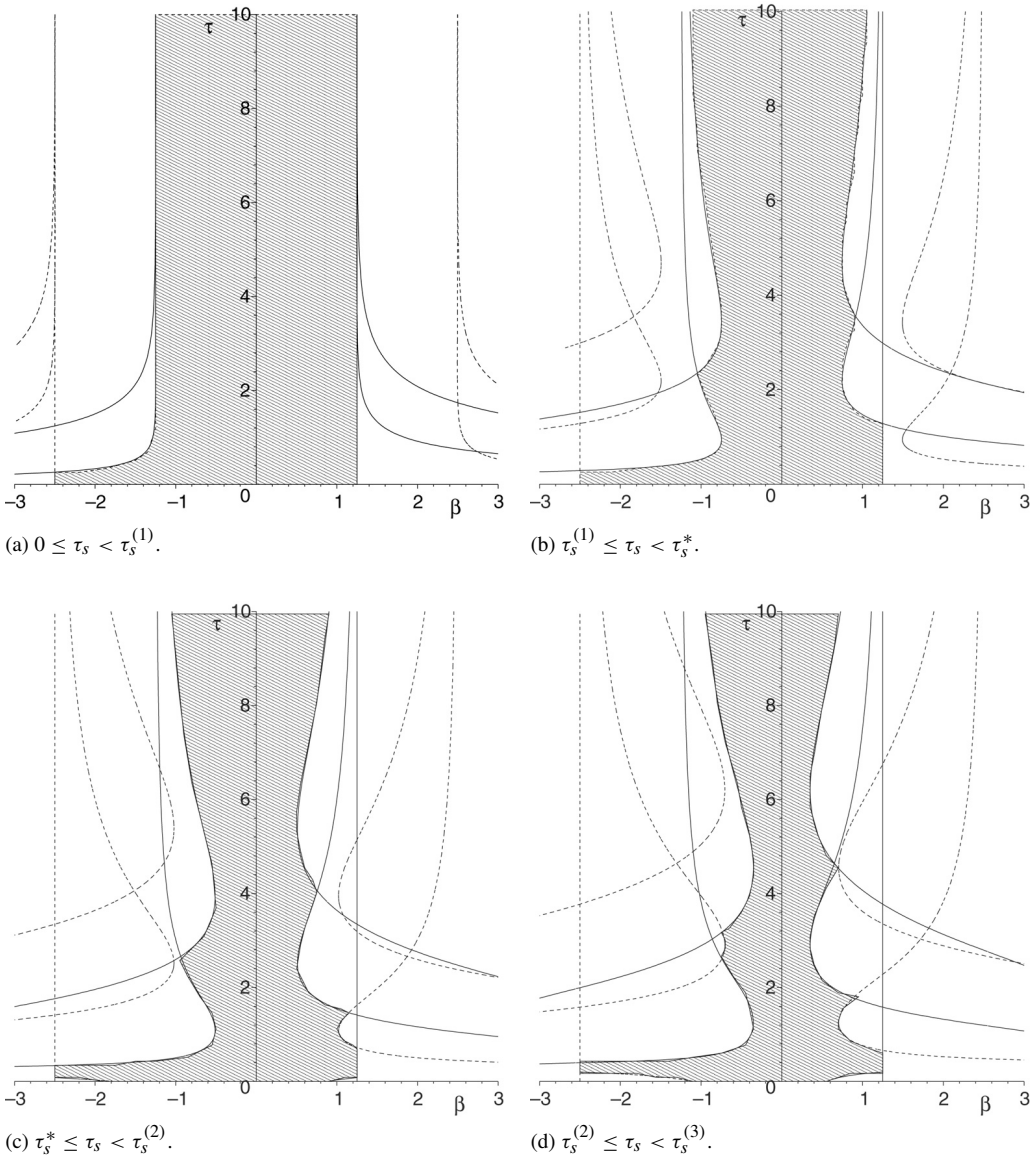

(a) $0 \le \tau_s < \tau_s^{(1)}$. (b) $\tau_s^{(1)} \le \tau_s < \tau_s^*$.

(c) $\tau_s^* \le \tau_s < \tau_s^{(2)}$. (d) $\tau_s^{(2)} \le \tau_s < \tau_s^{(3)}$.

Fig. 3.2. Region of stability of the trivial solution for $\alpha < -1$. Actual parameter values: $\alpha = -1.5$, $\tau_s = 0.3, 0.6, 0.8, 1$.

bifurcation parameter and the other parameters are fixed. See e.g. [36] where this is done for the standard Hopf bifurcation and [53] where it is done for the equivariant Hopf.

Consider first the standard bifurcations. Since these correspond to $\Delta_2(\lambda)$ having roots with zero real part, they are depicted by the solid curves and lines in Figs. 3.1 and 3.2. It is straightforward to check that these bifurcations give rise to synchronous solutions, i.e. solutions with $u_1(t) = u_2(t) = u_3(t)$. The criticality and type of bifurcation is determined by the nonlinearities f and g in (1.2). In [36], we used a centre manifold reduction to show that with $f = g = \tanh$ the Hopf bifurcation is supercritical if

$$\alpha(\tau_s - \tau)(\omega \sin(\omega\tau_s) - \cos(\omega\tau_s)) - \tau(1 + \omega^2) - 1 < 0,$$

and subcritical if this quantity is positive. Using a similar technique we can show that the steady state bifurcation is a supercritical pitchfork bifurcation if

$$1 + \alpha\tau_s + \tau(d - a) > 0,$$

and a subcritical pitchfork if this quantity is negative.

The equivariant bifurcations correspond to $\Delta_1(\lambda)$ having roots with zero real part, hence they are depicted by the dashed curves and line in Figs. 3.1 and 3.2. These bifurcations give rise to asynchronous solutions, i.e. solutions with $u_i(t) \ne u_j(t)$ for some $i \ne j$. More specifically, standard results [19,30,51] tell us that the equivariant Hopf bifurcations will give rise to eight branches of periodic orbits with period $\mathcal{P}$: two branches of phase-locked oscillations, $u_i(t) = u_{i-1}(t \pm \mathcal{P}/3)$; three branches of mirror-reflecting waves, $u_i(t) = u_j(t) \ne u_k(t)$ for some $i \ne j \ne k$; and three branches of standing waves, $u_i(t) = u_j(t + \mathcal{P}/2)$ for some pair $i \ne j$. Sections 5 and 6 will use perturbation theory to develop an approximation to the phase-locked periodic orbits and determine their stability

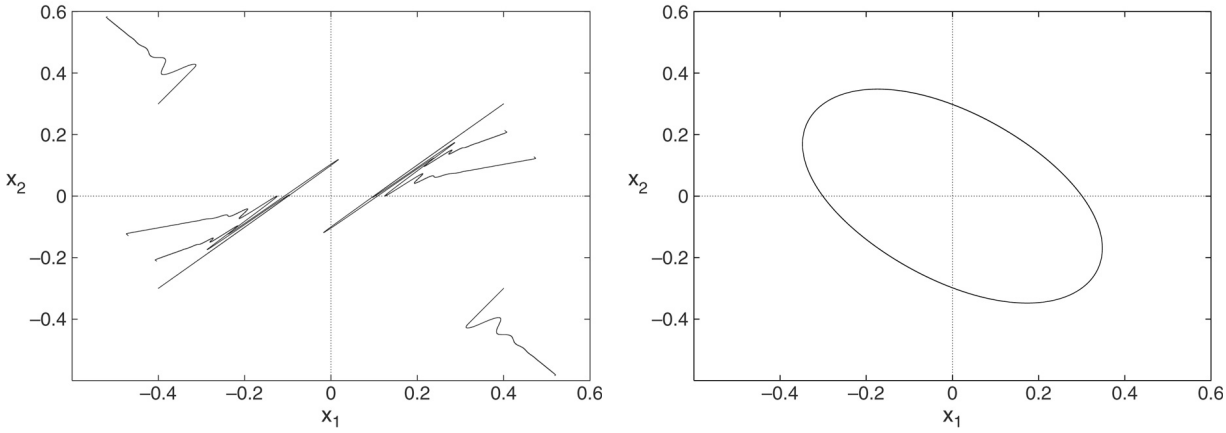

(a) Asynchronous equilibria $\alpha = 0.5$, $\tau_s = 0.7$, $\beta = -0.6$, $\tau = 1.5$. Parameter values correspond to Fig. 3.1(a).

(b) Asynchronous limit cycle $\alpha = -0.5$, $\tau_s = 3$, $\beta = -1.2$, $\tau = 0.1$.

Fig. 4.1. Numerical simulations of (1.2) with $f = g = \tanh$ showing stable asynchronous solutions.

when $f = g = \tanh$. We leave a discussion of the stability of the other branches to a future paper. Similarly, the equivariant steady state bifurcation will give rise to multiple branches of equilibria. For example, there will be three branches of "mirror reflecting" equilibria, $u_i(t) = u_j(t) = u^* \neq u_k(t) = v^*$, $i \neq j \neq k$, with

$$u^* = \alpha f(u^*) + \beta g(u^*) + \beta g(v^*),$$
$$v^* = \alpha f(v^*) + 2\beta g(u^*).$$

As mentioned before, we conjecture that all solutions will be asymptotically synchronous for parameter values such that no asynchronous pattern bifurcates from the trivial solution. Therefore, we formulate the following conjecture:

Conjecture 1. *If $|\beta| < |1-\alpha|$ and $\tau_s < \tau_s^{(1)}$ or if $|\beta| < \frac{1}{2}|1-\alpha|$ and $\tau_s < \tau_s^{(2)}$, then for all $\tau \geq 0, \alpha$, every solution of (1.2) is asymptotically synchronous.*

Desynchronization occurs when (1.2) possesses stable solutions $(u_1(t), u_2(t), u_3(t))$ with $u_j(t) \neq u_k(t)$ for some $j \neq k$ and some $t \geq 0$. The bifurcation analysis above gives indications of parameter values for which this can occur. In particular, desynchronization via equilibria can occur when $\beta < \alpha - 1$ and τ is sufficiently small (see Fig. 4.1(a)). Desynchronization via periodic orbits can occur when $\alpha < 0$, $\tau_s > \tau_s^*$, $\alpha - 1 < \beta < 0$ and τ is sufficiently small or when $\alpha < -\frac{1}{3}$, $\tau_s > \tau_s^{(2)}$ and $|\beta| < \frac{1}{2}(1-\alpha)$ (see Fig. 4.1(b)).

Multistability occurs when system (1.2) possesses multiple stable solutions. Due to the symmetry of the system, there will always be multistability when stable nontrivial solutions of (1.2) exist (the existence of one nontrivial solution implies the existence of a whole group orbit). We will focus instead on multistability which is *not* due to the symmetry of the system.

One way to induce such multistability is through bifurcation interactions. From the analysis in the previous section, it is clear that if $\tau_s > \tau_s^{(1)}$ then there can be intersection points of the curves $(\beta_H^{\pm}, \tau_{Hk}^{\pm}), k \geq 0$ with each other or with the line $\beta = \frac{1}{2}(1-\alpha)$ which lie on the boundary of the stability region. The former correspond to Hopf–Hopf interactions and the latter to Hopf–steady state interactions. If the corresponding bifurcations are supercritical, near the interaction points we may find coexistence of multiple stable synchronous solutions. Similarly, if $\tau_s > \tau_s^{(2)}$ then there can be intersection points of the curves $(\beta_{Hd}^{\pm}, \tau_{Hdk}^{\pm}), k \geq 0$ with each other or with the line $\beta = (\alpha - 1)$ which lie on the boundary of the stability region. Such points may lead to coexistence of multiple stable asynchronous solutions.

Most interestingly, if $\tau_s > \tau_s^{(2)}$, then there can be intersection points of the curves $(\beta_H^{\pm}, \tau_{Hk}^{\pm}), k \geq 0$ with the curves $(\beta_{Hd}^{\pm}, \tau_{Hdk}^{\pm}), k \geq 0$. These may lead to coexistence of stable synchronous and asynchronous oscillatory solutions. Such a situation is shown in Fig. 4.2(a). Near the intersection points of the curves $(\beta_{Hd}^{\pm}, \tau_{Hdk}^{\pm}), k \geq 0$ and the line $\beta = \frac{1}{2}(\alpha - 1)$, one may find coexistence of stable asynchronous limit cycles and stable synchronous equilibria. An example is shown in Fig. 4.2(b). Similarly, near the intersection points of the curves $(\beta_H^{\pm}, \tau_{Hk}^{\pm}), k \geq 0$ and the line $\beta = 1 - \alpha$, one may find coexistence of stable synchronous limit cycles and stable asynchronous equilibria.

5. Approximation to the phase-locked oscillation

Recall that the linearization of (1.2) about $(0, 0, 0)$ is given by

$$\dot{u}_j(t) = -u_j(t) + \alpha u_j(t - \tau_s) + \beta[u_{j-1}(t-\tau) + u_{j+1}(t-\tau)], \tag{5.1}$$

with j mod 3; and the associated characteristic equation is

$$S(\lambda) \stackrel{def}{=} \Delta_1^2(\lambda)\Delta_2(\lambda) = 0, \tag{5.2}$$

where

$$\Delta_1(\lambda) = \lambda + 1 - \alpha e^{-\lambda\tau_s} + \beta e^{-\lambda\tau},$$
$$\Delta_2(\lambda) = \lambda + 1 - \alpha e^{-\lambda\tau_s} - 2\beta e^{-\lambda\tau}.$$

As the parameters are varied, stability may be lost by a real root of the characteristic equation passing through zero, or by a pair

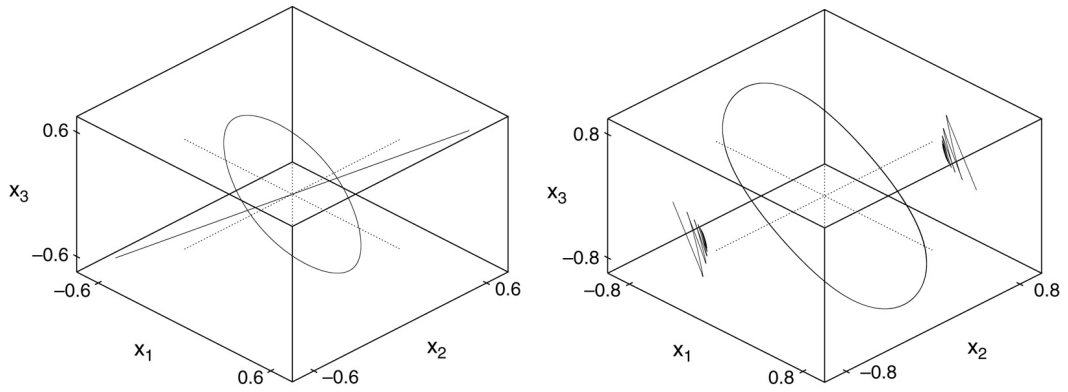

(a) Synchronous and asynchronous limit cycles. $\alpha = -1.5$, $\tau_s = 1.0$, $\beta = 1.0$, $\tau = 1.8$.

(b) Asynchronous limit cycle and synchronous equilibria. $\alpha = -1.5$, $\tau_s = 1.0$, $\beta = 1.3$, $\tau = 0.9$.

Fig. 4.2. Numerical simulations of (1.2) with $f = g = \tanh$ showing coexistence of synchronous and asynchronous solutions. Parameter values correspond to Fig. 3.2(c).

of complex conjugate roots passing through the imaginary axis. The former occurs when $\beta = \frac{1}{2}(1-\alpha)$, where the characteristic equation has a simple zero root, and when $\beta = \alpha - 1$, where the characteristic equation has a double zero root. The latter occurs if at least one of the following two situations occurs:

1. The characteristic equation has a simple pair of purely imaginary roots $\pm i\omega$ for parameter values such that $\Delta_2(\pm i\omega) = 0$.
2. The characteristic equation has a repeated (double) pair of purely imaginary roots $\pm i\omega$ for parameter values such that $\Delta_1(\pm i\omega) = 0$.

In the rest of this paper, we focus on the second case (see [36] for a discussion of the first case), showing that a Hopf bifurcation occurs under generic conditions and analyzing the stability of the resulting phase-locked oscillations.

Consider the factor (of the characteristic equation)

$$\Delta_1(\lambda) = \lambda + 1 - \alpha e^{-\lambda\tau_s} + \beta e^{-\lambda\tau},$$

and let $\lambda = i\omega$. This gives the two relationships between parameters α, β, τ_s, and τ

$$\begin{aligned} 1 - \alpha\cos(\omega\tau_s) + \beta\cos(\omega\tau) &= 0, \\ \omega + \alpha\sin(\omega\tau_s) - \beta\sin(\omega\tau) &= 0, \end{aligned} \tag{5.3}$$

which determine parameter values for which (5.2) has a pair of purely imaginary roots. Without loss of generality, we suppose that all the parameters are fixed except τ which will be the bifurcation parameter. Applying Theorem 1.1 on page 332 of [27], we proceed as follows. In (5.1), suppose that $\lambda = \lambda(\tau)$. Differentiating with respect to τ and solving for $\frac{d\lambda}{d\tau}$ gives

$$\begin{aligned} \frac{d\lambda}{d\tau} &= -\frac{\partial S}{\partial\tau} \Big/ \frac{\partial S}{\partial\lambda}, \\ &= -\left(\frac{\Delta_1(\lambda)\frac{\partial\Delta_2}{\partial\tau} + 2\Delta_2\frac{\partial\Delta_1}{\partial\tau}}{\Delta_1(\lambda)\frac{\partial\Delta_2}{\partial\lambda} + 2\Delta_2\frac{\partial\Delta_1}{\partial\lambda}} \right). \end{aligned} \tag{5.4}$$

Evaluating this at $\lambda = i\omega$ where $\Delta_1(i\omega) = 0$ then yields

$$\begin{aligned} \left(\frac{d\lambda}{d\tau}\bigg|_{\lambda=i\omega} \right) &= -\left(\frac{\partial\Delta_1}{\partial\tau} \Big/ \frac{\partial\Delta_1}{\partial\lambda} \right)\bigg|_{\lambda=i\omega} \\ &= \left(\frac{\beta\lambda e^{-\lambda\tau}}{1 + \alpha\tau_s e^{-\lambda\tau_s} - \beta\tau e^{-\lambda\tau}}\bigg|_{\lambda=i\omega} \right). \end{aligned}$$

From the above, we find that

$$\mathrm{Re}\left(\frac{d\lambda}{d\tau}\bigg|_{\lambda=i\omega} \right) = \frac{\beta\omega K_1\sin(\omega\tau) + \beta\omega K_2\cos(\omega\tau)}{K_1^2 + K_2^2},$$

where $K_1 = 1 + \alpha\tau_s\cos(\omega\tau_s) - \beta\tau\cos(\omega\tau)$ and $K_2 = \beta\tau\sin(\omega\tau) - \alpha\tau_s\sin(\omega\tau_s)$. Hence, the usual transversality condition is met if and only if

$$\beta\omega[\sin(\omega\tau) + \alpha\tau_s\sin(\omega(\tau - \tau_s))] \neq 0. \tag{5.5}$$

Summarizing the above discussions and applying the well-known (for details, see [51] and pp. 126 of [30]) *equivariant Hopf bifurcation theorem* for delay differential equations, we conclude that system (1.2) undergoes a Hopf bifurcation on the surfaces defined by (5.3) if condition (5.5) holds. Further, the particular symmetry of our model implies [51,28,19] that this Hopf bifurcation gives rise to phase-locked, standing, and mirror-reflecting waves.

Our ultimate goal is to study the stability of the bifurcating phase-locked oscillations. To do this, we must first construct an approximation to the bifurcating phase-locked solution. Our construction is based on a perturbation procedure together with an application of Fredholm alternative theory (see Sattinger [46] for details).

Before starting, we state some notation and assumptions. For clarity, we will consider a specific point on the bifurcation surface defined by (5.3), i.e. for a fixed α, β, τ_s we will assume there is a root $\lambda = i\omega_0$ of (5.2) when $\tau = \tau_0$, where τ_0 is implicitly defined by (5.3). Further, we must specify specific nonlinearities in (1.2), we thus take $f(x) = g(x) = \tanh(x)$.

Our construction begins by rescaling the variable t in (1.2) by setting $s = \omega(\epsilon)t$, where $\epsilon > 0$ is a small number. Then solutions which are $\frac{2\pi}{\omega}$ periodic in t will correspond to solutions which are 2π periodic in s. Let

$$x_j(s) = u_j\left(\frac{s}{\omega}\right), \quad j = 1, 2, 3. \tag{5.6}$$

System (1.2) then becomes

$$\omega\dot{x}_j(s) = -x_j(s) + \alpha f(x_j(s-\omega\tau_s)) + \beta[f(x_{j-1}(s-\omega\tau)) + f(x_{j+1}(s-\omega\tau))], \quad (5.7)$$

where j mod 3. Using the Taylor expansion of $f = g = \tanh$ in (5.7) gives

$$\begin{aligned}\omega\dot{x}_j(s) = {} & -x_j(s) + \alpha x_j(s-\omega\tau_s) \\ & + \beta[x_{j-1}(s-\omega\tau) + x_{j+1}(s-\omega\tau)] \\ & - \frac{1}{3}(\alpha x_j^3(s-\omega\tau_s) + \beta[x_{j-1}^3(s-\omega\tau) \\ & + x_{j+1}^3(s-\omega\tau)]) + \cdots, \end{aligned} \quad (5.8)$$

where j mod 3. We look for solutions of (5.8) in the form of a perturbation series:

$$\begin{aligned}\mathbf{X}(s,\epsilon) = {} & \epsilon\mathbf{x}_0 + \epsilon^2\mathbf{x}_1(s) + \epsilon^3\mathbf{x}_2(s) + \cdots \\ = {} & \epsilon\left\{\begin{pmatrix} x_{00}(s) \\ x_{10}(s) \\ x_{20}(s)\end{pmatrix} + \epsilon\begin{pmatrix} x_{01}(s) \\ x_{11}(s) \\ x_{21}(s)\end{pmatrix} + \epsilon^2\begin{pmatrix} x_{02}(s) \\ x_{12}(s) \\ x_{22}(s)\end{pmatrix} + \cdots\right\} \\ \stackrel{def}{=} {} & \begin{pmatrix} x_0(s) \\ x_1(s) \\ x_2(s)\end{pmatrix}. \end{aligned} \quad (5.9)$$

The periods of the oscillatory solutions of the nonlinear system will depend on the parameter τ, thus we perturb both the frequency and the delay as follows:

$$\begin{aligned}\omega &= \omega_0 + \epsilon\omega_1 + \epsilon^2\omega_2 + \cdots \\ \tau &= \tau_0 + \epsilon\tau_1 + \epsilon^2\tau_2 + \cdots, \end{aligned} \quad (5.10)$$

where τ_0 and ω_0 are as described above. From (5.9) and (5.10), we obtain

$$\begin{aligned}x_j(s-\omega\tau) = {} & \epsilon x_{j0}(s-\omega\tau) + \epsilon^2 x_{j1}(s-\omega\tau) \\ & + \epsilon^3 x_{j2}(s-\omega\tau) + \cdots, \end{aligned} \quad (5.11)$$

where

$$\begin{aligned}x_{ji}(s-\omega\tau) = {} & x_{ji}(s-\omega_0\tau_0) \\ & - \dot{x}_{ji}(s-\omega_0\tau_0)[\epsilon(\omega_1\tau_0 + \omega_0\tau_1) \\ & + \epsilon^2(\omega_2\tau_0 + \omega_1\tau_1 + \omega_0\tau_2) + \cdots] \\ & + \frac{1}{2}\ddot{x}_{ji}(s-\omega_0\tau_0)[\epsilon(\omega_1\tau_0 + \omega_0\tau_1) + \cdots]^2 \\ & + \cdots, \end{aligned} \quad (5.12)$$

with j mod 3, and $i = 0, 1, 2, \ldots$. Substituting (5.9), (5.11) and (5.12) into (5.8) gives

$$\begin{aligned}&\omega[\epsilon\dot{x}_{j0}(s) + \epsilon^2\dot{x}_{j1}(s) + \epsilon^3\dot{x}_{j2}(s) + \cdots] \\ &\quad = -x_{j0}(s) - x_{j1}(s) - x_{j2}(s) + \alpha[\epsilon x_{j0}(s-\omega\tau_s) \\ &\qquad + \epsilon^2 x_{j1}(s-\omega\tau_s) + \epsilon^3 x_{j2}(s-\omega\tau_s) + \cdots] \\ &\qquad + \epsilon\beta[x_{j-1\,0}(s-\omega\tau) + x_{j+1\,0}(s-\omega\tau)] \\ &\qquad + \epsilon^2\beta[x_{j-1\,1}(s-\omega\tau) + x_{j+1\,1}(s-\omega\tau)] \\ &\qquad + \epsilon^3\beta[x_{j-1\,2}(s-\omega\tau) + x_{j+1\,2}(s-\omega\tau)] + \cdots. \end{aligned} \quad (5.13)$$

It is to be noted that x_0, x_1, x_2 are 2π periodic in the variable s. Using the expansions in (5.8) and employing (5.9)–(5.14), we obtain the following equations for the first and second orders of the perturbation expansion

$$L_j[\mathbf{x}_0] = 0, \quad (5.14)$$

$$\begin{aligned}L_j[\mathbf{x}_1] = {} & -\omega_1\dot{x}_{j0}(s) - \alpha\omega_1\dot{x}_{j0}(s-\omega_0\tau_s)\tau_s \\ & - \beta(\omega_0\tau_1 + \omega_1\tau_0)[\dot{x}_{j+1\,0}(s-\omega_0\tau_0) \\ & + \dot{x}_{j-1\,0}(s-\omega_0\tau_0)], \end{aligned} \quad (5.15)$$

where j mod 3 and the operator $L_j(\cdot)$ is defined by

$$\begin{aligned}L_j[\mathbf{x}_k] \stackrel{def}{=} {} & \omega_0\dot{x}_{jk}(s) + x_{jk}(s) - \alpha x_{jk}(s-\omega_0\tau_s) \\ & - \beta[x_{j+1\,k}(s-\omega_0\tau_0) + x_{j-1\,k}(s-\omega_0\tau_0)]. \end{aligned}$$

Note that the system (5.14) is identical to the linear system (3.1). Since we are interested in phase-locked oscillations, we choose the solution

$$\mathbf{x}_0(s) = \begin{pmatrix} x_{00}(s) \\ x_{10}(s) \\ x_{20}(s)\end{pmatrix} = \begin{pmatrix} \cos(s) \\ \cos\left(s + \dfrac{2\pi}{3}\right) \\ \cos\left(s + \dfrac{4\pi}{3}\right)\end{pmatrix}. \quad (5.16)$$

The next step is to compute $[x_{01}(s),\ x_{11}(s),\ x_{21}(s)]^{\mathrm{T}}$ as a 2π periodic solution of a nonhomogeneous linear system of ODEs (5.15), for suitable ω_1 and τ_1. A necessary and sufficient condition for the existence of such a solution is provided by the *Fredholm alternative theory* [24]: that the nonhomogeneous terms of (5.15) are orthogonal to all phase-locked 2π periodic solutions of the system adjoint to the homogeneous system associated with (5.15). This adjoint system is given by [24]

$$\begin{aligned}&\omega_0\dot{x}_{j\,1}(s) - x_{j\,1}(s) + \alpha x_{j\,1}(s+\omega_0\tau_s) \\ &\quad + \beta[x_{j+1\,1}(s+\omega_0\tau_0) + x_{j-1\,1}(s+\omega_0\tau_0)] = 0, \end{aligned} \quad (5.17)$$

where j mod 3. We assume that the solutions of the adjoint system (5.17) are of the form

$$\begin{pmatrix} F_0 \\ F_1 \\ F_2\end{pmatrix} e^{\lambda s} \in P(2\pi), \quad F_0, F_1, F_2 \in \mathbb{C}, \quad (5.18)$$

where $P(2\pi)$ denotes functions which are 2π periodic. Under conditions (5.3), one pair of eigenvalues of the adjoint system (5.17) is given by $\lambda = \pm\mathrm{i}$. The corresponding eigenvectors for the phase-locked solutions are given by $\mathbf{V}$ and $\overline{\mathbf{V}}$, with $\mathbf{V} = [1, e^{\mathrm{i}\frac{2\pi}{3}}, e^{\mathrm{i}\frac{4\pi}{3}}]^{\mathrm{T}}$. Therefore, the space of complex-valued, phase-locked, 2π-periodic solutions of (5.17) is spanned by $e^{\mathrm{i}t}\mathbf{V}, e^{\mathrm{i}t}\overline{\mathbf{V}}$. and a basis for the real-valued, phase-locked,

2π-periodic solutions (5.17) is given by:

$$\xi^{(1)}(s) = \begin{pmatrix} \cos(s) \\ \cos\left(s + \frac{2\pi}{3}\right) \\ \cos\left(s - \frac{2\pi}{3}\right) \end{pmatrix}, \qquad \xi^{(2)}(s) = \begin{pmatrix} -\sin(s) \\ -\sin\left(s + \frac{2\pi}{3}\right) \\ -\sin\left(s - \frac{2\pi}{3}\right) \end{pmatrix}. \tag{5.19}$$

We are thus led to the following

Theorem 6. *A necessary and sufficient condition for the solvability of the nonhomogeneous equation (5.15) is that its nonhomogeneous terms,* $\mathbf{F}(s)$*, satisfy*

$$\int_0^{2\pi} \xi^{(1)}(s) \cdot \mathbf{F}(s)\,\mathrm{d}s = 0 = \int_0^{2\pi} \xi^{(2)}(s) \cdot \mathbf{F}(s)\,\mathrm{d}s,$$

where $\{\xi^{(1)}(s),\ \xi^{(2)}(s)\}$ *is the basis of the solution space of (5.17).*

Applying Theorem 6, we can set up a system of two equations in τ_1 and ω_1, viz.

$$\int_0^{2\pi} \xi^{(1)}(s) \cdot \{\text{RHS of (5.15)}\}(s)\,\mathrm{d}s = 0 = \int_0^{2\pi} \xi^{(2)}(s) \cdot \{\text{RHS of (5.15)}\}(s)\,\mathrm{d}s,$$

giving

$$\beta(\omega_1\tau_s - \omega_0\tau_1 - \omega_1\tau_0)\sin(\omega_0\tau_0) - \omega_0\omega_1\tau_s = 0,$$
$$\beta(\omega_1\tau_s - \omega_0\tau_1 - \omega_1\tau_0)\cos(\omega_0\tau_0) + \omega_1(1+\tau_s) = 0.$$

These two equations are then solved to obtain $\omega_1 = 0 = \tau_1$, which are then plugged back into (5.15) to give the system

$$L_j[\mathbf{x}_1] = 0, \quad j \bmod 3, \tag{5.20}$$

which is the linear homogeneous system associated with (5.15), and is identical to systems (5.14) and (5.1). Thus the only phase-locked 2π periodic solution is either the trivial solution or the same as $\mathbf{x}_0(s)$ up to a phase shift. We choose the nontrivial solution

$$\mathbf{x}_1(s) = \begin{pmatrix} x_{01}(s) \\ x_{11}(s) \\ x_{21}(s) \end{pmatrix} = \begin{pmatrix} \cos(s+\delta) \\ \cos\left(s + \frac{2\pi}{3} + \delta\right) \\ \cos\left(s + \frac{4\pi}{3} + \delta\right) \end{pmatrix}, \quad \text{for some } \delta. \tag{5.21}$$

The next set of equations, i.e. governing $[x_{02}(s), x_{12}(s), x_{22}(s)]^{\mathrm{T}}$, can be obtained by extracting the coefficients of ϵ^3 in (5.8). We obtain the following:

$$\begin{aligned} L_j[\mathbf{x}_2] = {} & -\omega_2\dot{x}_{j0}(s) - \alpha\dot{x}_{j0}(s-\omega_0\tau_s)\omega_2\tau_s \\ & - \beta[\dot{x}_{j+1\,0}(s-\omega_0\tau_0) + \dot{x}_{j-1\,0}(s-\omega_0\tau_0)] \\ & \times (\omega_0\tau_2 + \omega_2\tau_0) - \frac{1}{3}\alpha x_{j0}^3(s-\omega_0\tau_s) \\ & - \frac{1}{3}\beta[x_{j-1\,0}^3(s-\omega_0\tau_0) + x_{j+1\,0}^3(s-\omega_0\tau_0)], \\ & j \bmod 3. \end{aligned} \tag{5.22}$$

Let us now denote the RHS of (5.22) by $\mathbf{F}(s)$. Then, invoking the Fredholm solvability condition on (5.22) leads to

$$\int_0^{2\pi} \xi^{(1)}(s) \cdot \mathbf{F}(s)\,\mathrm{d}s = 0 = \int_0^{2\pi} \xi^{(2)}(s) \cdot \mathbf{F}(s)\,\mathrm{d}s,$$

which gives the system

$$\beta(\omega_2\tau_s - \omega_2\tau_0 - \omega_0\tau_2)\sin(\omega_0\tau_0) - \omega_0\omega_2\tau_s - \frac{1}{4} = 0,$$
$$\beta(\omega_2\tau_s - \omega_0\tau_2 - \omega_2\tau_0)\cos(\omega_0\tau_0) + \omega_2(1+\tau_s) + \frac{1}{4}\omega_0 = 0.$$

This system is solved to obtain non-trivial expressions for $\omega_2 = \omega_2(\alpha, \beta, \omega_0, \tau_s, \tau_0)$ and $\tau_2 = \tau_2(\alpha, \beta, \omega_0, \tau_s, \tau_0)$, as shown below:

$$\omega_2 = \frac{1}{4}\left[\frac{\omega_0\sin(\omega_0\tau_0) - \cos(\omega_0\tau_0)}{\omega_0\tau_s\cos(\omega_0\tau_0) + (1+\tau_s)\sin(\omega_0\tau_0)}\right], \tag{5.23}$$

and

$$\tau_2 = \frac{-\Gamma(\omega_0, \tau_0, \tau_s, \beta)}{4\beta\omega_0[\omega_0\tau_s\cos(\omega_0\tau_0) + \sin(\omega_0\tau_0) + \tau_s\sin(\omega_0\tau_0)]}, \tag{5.24}$$

where

$$\begin{aligned} \Gamma(\omega_0, \tau_0, \tau_s, \beta) \overset{def}{=} {} & 1 + \tau_s(1+\omega_0^2) + \beta(\tau_s - \tau_0) \\ & \times [\cos(\omega_0\tau_0) - \omega_0\sin(\omega_0\tau_0)]. \end{aligned} \tag{5.25}$$

Using (5.9) and (5.10) we can now write down the approximate solution of (5.8):

$$\mathbf{X}(s) = \sqrt{\left(\frac{\tau - \tau_0}{\tau_2}\right)}\mathbf{x}_0(s) + \frac{\tau - \tau_0}{\tau_2}\mathbf{x}_1(s) + \cdots, \tag{5.26}$$

where $\mathbf{x}_0(s)$ and $\mathbf{x}_1(s)$ are given in (5.16) and (5.21), respectively, and τ_2 is given in (5.24). Using the values of ω_2 and τ_2 obtained above, the approximation $\mathbf{x}_2(s)$ may be computed from (5.22) by the method of undetermined coefficients.

6. Stability of phase-locked oscillations

In the previous section, we constructed an approximation to the phase-locked oscillatory solution resulting from the double root single Hopf bifurcation of periodic solutions of (1.2). We now focus on determining the stability of this solution. The discussion of stability of periodic solutions involves the computation of *Floquet exponents*.

We rewrite the solution (5.26) of system (5.8) in the form

$$\mathbf{X}(s,\epsilon) = \epsilon\{\mathbf{x}_0(s) + \epsilon\mathbf{x}_1(s) + \epsilon^2\mathbf{x}_2(s) + \cdots\} = \epsilon\begin{pmatrix} T_0(s) \\ T_1(s) \\ T_2(s) \end{pmatrix}. \tag{6.1}$$

To study the stability of the periodic solution in (6.1), we proceed by considering the corresponding Poincaré–Lindstedt series expansion. Let $[x_0, x_1, x_2]^{\mathrm{T}}$ be a given solution of (5.7). Define the deviations R_0, R_1, and R_2 by the following:

$$\begin{pmatrix} x_0 \\ x_1 \\ x_2 \end{pmatrix} = \epsilon\begin{pmatrix} T_0 \\ T_1 \\ T_2 \end{pmatrix} + \begin{pmatrix} R_0 \\ R_1 \\ R_2 \end{pmatrix}. \tag{6.2}$$

Substituting $[x_0, x_1, x_2]^{\mathrm{T}}$ in (5.7) gives the following system

$$\begin{aligned}\omega\frac{\mathrm{d}}{\mathrm{d}s}[\epsilon T_j + R_j] = {} & -\epsilon T_j - R_j \\ & + \alpha f[\epsilon T_j(s-\omega\tau_s) + R_j(s-\omega\tau_s)] \\ & + \beta\{g[\epsilon T_{j-1}(s-\omega\tau) + R_{j-1}(s-\omega\tau)] \\ & + g[\epsilon T_{j+1}(s-\omega\tau) + R_{j+1}(s-\omega\tau)]\},\end{aligned} \tag{6.3}$$

where j mod 3. Since $\epsilon[T_0(s), T_1(s), T_2(s)]^{\mathrm{T}}$ is a solution of (5.7), we have

$$\begin{aligned}\epsilon\omega\frac{\mathrm{d}T_j}{\mathrm{d}s} + \epsilon T_j = {} & \alpha f[\epsilon T_j(s-\omega\tau_s)] + \beta\{g[\epsilon T_{j-1}(s-\omega\tau)] \\ & + g[\epsilon T_{j+1}(s-\omega\tau)]\},\end{aligned} \tag{6.4}$$

where j mod 3. Then, using $f = g = \tanh$ and

$$\begin{aligned}\tanh(\epsilon u + v) &= \tanh(\epsilon u) + \operatorname{sech}^2(\epsilon u)v \\ &= \tanh(\epsilon u) + (1 - \epsilon^2 u^2 + O(\epsilon^4))v\end{aligned}$$

together with (6.4), we can simplify (6.3) to obtain:

$$\begin{aligned}\omega\frac{\mathrm{d}R_j}{\mathrm{d}s} + R_j = {} & \alpha R_j(s-\omega\tau_s) \\ & + \beta R_{j-1}(s-\omega\tau) + \beta R_{j+1}(s-\omega\tau) \\ & - \epsilon^2\{\alpha T_j^2(s-\omega\tau_s)R_j(s-\omega\tau_s) \\ & + \beta[T_{j-1}^2(s-\omega\tau)R_{j-1}(s-\omega\tau) \\ & + T_{j+1}^2(s-\omega\tau)R_{j+1}(s-\omega\tau)]\} + \cdots,\end{aligned} \tag{6.5}$$

with j mod 3.

Now the stability of $\epsilon[T_0, T_1, T_2]^{\mathrm{T}}$ in (5.7) is equivalent to that of the trivial solution of (6.5), thus we let

$$\begin{pmatrix} \tilde{R}_0(s) \\ \tilde{R}_1(s) \\ \tilde{R}_2(s) \end{pmatrix} = \mathrm{e}^{\eta s}\begin{pmatrix} r_0(s) \\ r_1(s) \\ r_2(s) \end{pmatrix},$$

$$r_0(s), r_1(s), r_2(s) \in P(2\pi) \text{ in s.} \tag{6.6}$$

Following the usual convention, we term η the *Floquet exponent* and $\mathrm{e}^{2\eta\pi}$ the *Floquet multiplier*. The stability of the trivial solution of (6.5) will depend on the sign of the real part of η. Perturbing η via

$$\eta = \epsilon\eta_1 + \epsilon^2\eta_2 + \cdots, \tag{6.7}$$

our task is to find an approximate value of η by computing η_1 and η_2.

To do this, we must find an expression for the $r_j(s)$ in (6.6). Returning to (6.4), differentiating with respect to s and expanding the result in a Taylor series gives:

$$\begin{aligned}\omega\frac{\mathrm{d}}{\mathrm{d}s}\left(\frac{\mathrm{d}T_j}{\mathrm{d}s}\right) + \frac{\mathrm{d}T_j}{\mathrm{d}s} = {} & \alpha\frac{\mathrm{d}T_j}{\mathrm{d}s}(s-\omega\tau_s) + \beta\left[\frac{\mathrm{d}T_{j-1}}{\mathrm{d}s}(s-\omega\tau)\right. \\ & \left. + \frac{\mathrm{d}T_{j+1}}{\mathrm{d}s}(s-\omega\tau)\right] \\ & - \epsilon^2\left\{\alpha T_j^2(s-\omega\tau_s)\frac{\mathrm{d}T_j}{\mathrm{d}s}(s-\omega\tau_s)\right. \\ & + \beta T_{j-1}^2(s-\omega\tau)\frac{\mathrm{d}T_{j-1}}{\mathrm{d}s}(s-\omega\tau) \\ & \left. + \beta T_{j+1}^2(s-\omega\tau)\frac{\mathrm{d}T_{j+1}}{\mathrm{d}s}(s-\omega\tau)\right\} \\ & + \cdots,\end{aligned} \tag{6.8}$$

where j mod 3. Comparing the system (6.8) with (6.5), we see that, to $O(\epsilon^2)$, $[\frac{\mathrm{d}T_0}{\mathrm{d}s}, \frac{\mathrm{d}T_1}{\mathrm{d}s}, \frac{\mathrm{d}T_2}{\mathrm{d}s}]^{\mathrm{T}}$ is also a solution of (6.5). We thus look for the $r_j(s)$ in the form:

$$\begin{aligned}r_j(s) &= b(\epsilon)\frac{\mathrm{d}T_j}{\mathrm{d}s} + \tilde{r}_j(s), \\ &= b(\epsilon)\frac{\mathrm{d}T_j}{\mathrm{d}s} + r_{j0}(s) + \epsilon r_{j1}(s) + \epsilon^2 r_{j2}(s) + \cdots,\end{aligned} \tag{6.9}$$

where j mod 3, $r_{ji} \in P(2\pi)$ for all $i = 0, 1, 2, \ldots$, and

$$b(\epsilon) = b_0 + \epsilon b_1 + \epsilon^2 b_2 + \cdots. \tag{6.10}$$

We supply (6.6) in (6.5) to get a new system of equations in r_0, r_1, and r_2, namely,

$$\begin{aligned}\omega\eta r_j(s) + \omega\frac{\mathrm{d}r_j}{\mathrm{d}s} + r_j(s) = {} & \alpha\mathrm{e}^{-\eta\omega\tau_s}r_j(s-\omega\tau_s) \\ & + \beta\mathrm{e}^{-\eta\omega\tau}r_{j-1}(s-\omega\tau) + \beta\mathrm{e}^{-\eta\omega\tau}r_{j+1}(s-\omega\tau) \\ & - \epsilon^2\left[\alpha T_j^2(s-\omega\tau_s)\mathrm{e}^{-\eta\omega\tau_s}r_j(s-\omega\tau_s)\right. \\ & + \beta T_{j-1}^2(s-\omega\tau)\mathrm{e}^{-\eta\omega\tau}r_{j-1}(s-\omega\tau) \\ & \left. + \beta T_{j+1}^2(s-\omega\tau)\mathrm{e}^{-\eta\omega\tau}r_{j+1}(s-\omega\tau)\right] + \cdots,\end{aligned} \tag{6.11}$$

with j mod 3. Incorporating the fact that $[\frac{\mathrm{d}T_0}{\mathrm{d}s}, \frac{\mathrm{d}T_1}{\mathrm{d}s}, \frac{\mathrm{d}T_2}{\mathrm{d}s}]^{\mathrm{T}}$ is a solution of the system (6.8), we substitute (6.9) in (6.11) to get the following system in $\tilde{r}_0$, $\tilde{r}_1$, and $\tilde{r}_2$:

$$\begin{aligned}&\omega\eta b\frac{\mathrm{d}T_j}{\mathrm{d}s} + \omega\eta\tilde{r}_j(s) + \omega\frac{\mathrm{d}\tilde{r}_j}{\mathrm{d}s} + \tilde{r}_j = H_j[\mathbf{T}_j, \tilde{\mathbf{r}}_j], \\ &\quad j \text{ mod } 3,\end{aligned} \tag{6.12}$$

where the operator represented by $H_j[\cdot,\cdot]$ is given in the Appendix,

$$\begin{aligned}\tilde{r}_j(s-\omega\tau) = {} & r_{j0}(s-\omega\tau) + \epsilon r_{j1}(s-\omega\tau) \\ & + \epsilon^2 r_{j2}(s-\omega\tau) + \cdots,\end{aligned} \tag{6.13}$$

with j mod 3; and for each i,

$$\begin{aligned} r_{ji}(s-\omega\tau) &= r_{ji}(s-\omega_0\tau_0) \\ &\quad -\dot r_{ji}(s-\omega_0\tau_0)[\epsilon(\omega_1\tau_0+\omega_0\tau_1) \\ &\quad +\epsilon^2(\omega_2\tau_0+\omega_1\tau_1+\omega_0\tau_2)+\cdots] \\ &\quad +\frac{1}{2}\ddot r_{ji}(s-\omega_0\tau_0)[\epsilon(\omega_1\tau_0+\omega_0\tau_1)+\cdots]^2 \\ &\quad +\cdots, \end{aligned} \tag{6.14}$$

and

$$\begin{aligned} r_{ji}(s-\omega\tau_s) &= r_{ji}(s-\omega_0\tau_s)-\dot r_{ji}(s-\omega_0\tau_s) \\ &\quad \times[\epsilon\omega_1+\epsilon^2\omega_2+\cdots]\tau_s+\frac{1}{2}\ddot r_{ji}(s-\omega_0\tau_s) \\ &\quad \times[\epsilon\omega_1\tau_s+\epsilon^2\omega_2\tau_s+\cdots]^2+\cdots. \end{aligned} \tag{6.15}$$

Finally, we use the following series, with ω and τ given by (5.10) where $\omega_1 = 0 = \tau_1$:

$$\begin{aligned} \mathrm{e}^{-\eta\omega\tau} &= 1-\epsilon\eta_1\omega_0\tau_0+\epsilon\left[-\eta_2\omega_0\tau_0+\frac{1}{2}\eta_1^2\omega_0^2\tau_0^2\right] \\ &\quad -\epsilon^3\left[\eta_1\omega_0\tau_2+\eta_1\omega_2\tau_0+\eta_3\omega_0\tau_0+\frac{1}{6}\eta_1^3\omega_0^3\tau_0^3\right] \\ &\quad +\cdots, \end{aligned}$$

and

$$\begin{aligned} \mathrm{e}^{-\eta\omega\tau_s} &= 1-\epsilon\tau_s\eta_1\omega_0+\epsilon^2\left[\frac{1}{2}\tau_s^2\eta_1^2\omega_0^2-\tau_s\eta_2\omega_0\right] \\ &\quad +\epsilon^3\left[\frac{1}{2}\tau_s^2\eta_1\eta_2\omega_0^2-\tau_s(\eta_1\omega_2+\eta_3\omega_0)\right. \\ &\quad \left.-\frac{1}{6}\tau_s^3\eta_1^3\omega_0^3\right]+\cdots \end{aligned}$$

as well as the series in (5.9), (6.5), (6.7), (6.9) and (6.10) in (6.12); we then extract coefficients of ϵ^0 and ϵ^1 to get the following two systems of equations, respectively:

$$L_j[\mathbf{r}_0] = 0, \quad j \bmod 3, \tag{6.16}$$

and

$$\begin{aligned} L_j[\mathbf{r}_1] &= -\omega_0\eta_1 b_0\dot x_{j0}(s)-\omega_0\eta_1 r_{j0}(s) \\ &\quad -\alpha\tau_s\eta_1\omega_0\{b_0\dot x_{j0}(s-\omega_0\tau_s)+r_{j0}(s-\omega_0\tau_s)\} \\ &\quad -\beta\eta_1\omega_0\tau_0\{b_0\dot x_{j-1\,0}(s-\omega_0\tau_0)+r_{j-1\,0}(s-\omega_0\tau_0)\} \\ &\quad -\beta\eta_1\omega_0\tau_0\{b_0\dot x_{j+1\,0}(s-\omega_0\tau_0)+r_{j+1\,0}(s-\omega_0\tau_0)\}, \end{aligned} \tag{6.17}$$

where $L_j(\cdot)$ is given by (5.14), the $x_{ij}(s)$ are given by (5.16) and (5.21), and $j \bmod 3$. The system (6.16) is identical to (5.20), and hence a phase-locked 2π periodic solution of (6.16) is given by

$$\begin{bmatrix} r_{00}(s) \\ r_{10}(s) \\ r_{20}(s) \end{bmatrix} = \begin{bmatrix} \cos(s) \\ \cos\left(s+\dfrac{2\pi}{3}\right) \\ \cos\left(s+\dfrac{4\pi}{3}\right) \end{bmatrix}.$$

As discussed in Section 5, the necessary and sufficient conditions for the existence of a solution of (6.17) is that the RHS of (6.17) satisfy the Fredholm solvability conditions:

$$\begin{aligned} &\int_0^{2\pi}\xi^{(1)}(s)\cdot\{\text{RHS of (6.17)}\}(s)\,\mathrm{d}s = 0 \\ &\quad =\int_0^{2\pi}\xi^{(2)}(s)\cdot\{\text{RHS of (6.17)}\}(s)\,\mathrm{d}s, \end{aligned}$$

where $\xi^{(1)}(s)$ and $\xi^{(2)}(s)$ are as in Theorem 6. This yields the two coupled equations in η_1 and b_0:

$$\begin{aligned} &\omega_0\eta_1[V_1\sin(\omega_0\tau_s)+V_2\cos(\omega_0\tau_s)+V_3] = 0, \\ &\omega_0\eta_1[W_1\sin(\omega_0\tau_s)+W_2\cos(\omega_0\tau_s)+W_3] = 0, \end{aligned}$$

where

$$\begin{aligned} V_1 &= -\tau_0\alpha b_0+\alpha\tau_s b_0-\alpha\tau_s\sqrt{3}+\alpha\tau_0\sqrt{3}, \\ V_2 &= -\tau_0\alpha-\tau_0 b_0\alpha\sqrt{3}+\alpha\tau_s b_0\sqrt{3}+\alpha\tau_s, \\ V_3 &= 1+\tau_0\omega_0\sqrt{3}-\omega_0\tau_0 b_0+b_0\sqrt{3}+\tau_0 b_0\sqrt{3}+\tau_0, \\ W_1 &= \tau_0\alpha+\tau_0\alpha b_0\sqrt{3}-\alpha\tau_s b_0\sqrt{3}-\alpha\tau_s, \\ W_2 &= -\tau_0 b_0\alpha+\tau_0\alpha\sqrt{3}+\alpha\tau_s b_0-\alpha\tau_s\sqrt{3}, \\ W_3 &= b_0-\sqrt{3}+\tau_0 b_0+\omega_0\tau_0-\tau_0\sqrt{3}+\tau_0 b_0\omega_0\sqrt{3}. \end{aligned}$$

The above equations are solved using the symbolic computation language MAPLE, to find that $\eta_1 = 0$ and b_0 is arbitrary. For this η_1, we can simplify (6.17) to

$$L_j[\mathbf{r}_1] = 0, \quad j \bmod 3. \tag{6.18}$$

Since $\eta_1 = 0$, it is found that the equations governing r_{02}, r_{12} and r_{22} do not involve r_{01}, r_{11} and r_{21}. To solve for η_2 and b_0, we consider the equations which are obtained by comparing the coefficients of ϵ^2 in (6.12):

$$G_j[\mathbf{r}_2,\mathbf{x}_2] = M_j[\mathbf{r}_0,\mathbf{x}_0,\mathbf{x}_1], \tag{6.19}$$

where $j \bmod 3$, the operator $G_j[\cdot,\cdot]$ is defined by

$$\begin{aligned} G_j[\mathbf{r}_2,\mathbf{x}_2] &= \omega_0\dot r_{j2}(s)+r_{j2}(s) \\ &\quad -\alpha b_0\dot x_{j2}(s-\omega_0\tau_s)-\alpha r_{j2}(s-\omega_0\tau_s) \\ &\quad -\beta[b_0\dot x_{j-1\,2}(s-\omega_0\tau_0)+r_{j-1\,2}(s-\omega_0\tau_0)] \\ &\quad -\beta[b_0\dot x_{j+1\,2}(s-\omega_0\tau_0)+r_{j+1\,2}(s-\omega_0\tau_0)] \\ &\quad +b_0[\alpha\dot x_{j2}(s-\omega_0\tau_s)+\beta\dot x_{j-1\,2}(s-\omega_0\tau_0) \\ &\quad +\beta\dot x_{j+1\,2}(s-\omega_0\tau_0)], \end{aligned}$$

and the operator $M_j[\cdot,\cdot,\cdot]$ is given in the Appendix. Applying the Fredholm solvability condition to the system (6.19), and substituting for ω_2 and τ_2 from (5.23) and (5.24), we obtain complicated expressions for η_2 and b_0 of the form

$$\begin{aligned} \eta_2 &= \eta_2(\alpha,\beta(\omega_0,\alpha,\tau_s),\omega_0,\tau_s,\tau_0(\omega_0,\alpha,\tau_s)), \\ b_0 &= b_0(\alpha,\beta(\omega_0,\alpha,\tau_s),\omega_0,\tau_s,\tau_0(\omega_0,\alpha,\tau_s)). \end{aligned} \tag{6.20}$$

Now, $\epsilon^2\eta_2$ is the leading order term of the Floquet exponent. Recall that, given α,ω_0,τ_s, the parameters β and τ_0 are determined from Eq. (5.3). Thus we need to determine the sign of this exponent as the parameters (α,τ_s) are continuously varied. Due to the complexity of the expressions, we use symbolic computation to get some insight into the sign of the exponent η_2.

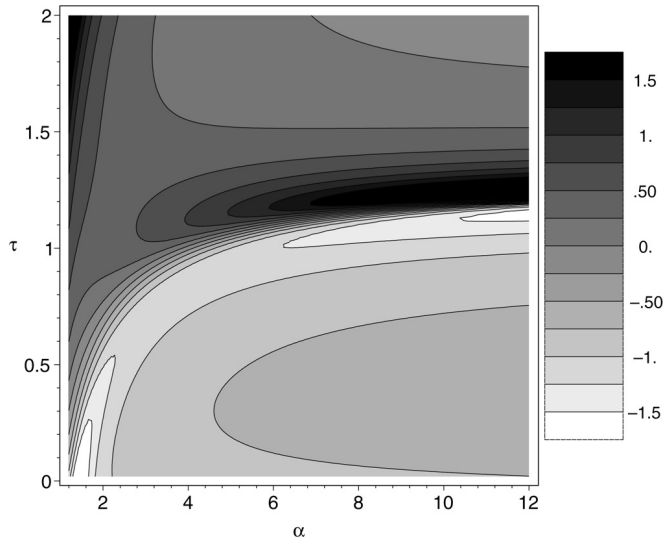

Fig. 6.1. A contour plot of the Floquet exponent $\eta_2[\alpha, \beta(\omega_0, \alpha, \tau_s), \omega_0, \tau_s, \tau_0(\omega_0, \alpha, \tau_s)]$ in the (α, τ_s) parameter space for fixed $\omega_0 = 0.6$. The parameters β and τ_0 are given by Eq. (5.3).

Fig. 6.1 shows a contour plot of η_2 in the (α, τ_s) parameter space, for fixed $\omega_0 = 0.6$. It is clear from Fig. 6.1 that, for the given range of parameter values, the stability of the phase-locked oscillation changes. When $\eta < 0$, bifurcating phase-locked oscillation is unstable, otherwise it is stable.

7. Conclusions and remarks

Gopalsamy and Leung [21] considered a simple system of two coupled neurons with a single discrete delay, and established that, for some parameter values, the approximations to periodic oscillations are stable. Their conclusion could have been much stronger had they not fixed their parameters c_1 and c_2 (pp. 412 of [21]). The local stability of a scalar version of (1.2) has been studied in [4]. Following this, Shayer and Campbell in [47] considered a system of two coupled neurons with multiple time delays and showed that the trivial equilibrium may lose stability via a pitchfork bifurcation, a Hopf bifurcation or one of three types of codimension two bifurcations. Multistability near the latter bifurcations was predicted and confirmed using centre manifold theory and numerical simulations. Furthermore Wu et al. [53] have conducted a rigorous and insightful study of (1.2) with $\tau_s = \tau$.

In this article, we studied the model (1.2) with $\tau_s \neq \tau$. We have extended many of the synchronization and global stability results of Wu et al. [53] to this case. Further, we used techniques similar to those of Shayer and Campbell to analyze the local stability and bifurcations of the trivial solution. This enabled us to study synchronization/desynchronization due to bifurcation and multistability due to bifurcation interactions. Finally, we extended the perturbation approach of Gopalsamy and Leung [21] to our model, yielding some interesting insight into the stability of phase-locked oscillations resulting from a D_3 equivariant Hopf bifurcation of (1.2). The technique of Gopalsamy and Leung seems to be less computationally challenging relative to the usual centre manifold approach. The obvious advantage of the centre manifold approach, *if successfully applied*, is that it would characterize criticality of the Hopf bifurcation in a very general setting.

One of the key conclusions to be drawn from this study is that change of the stability of the bifurcating phase-locked solutions can be easily achieved by varying the parameters α and τ_s, for fixed ω_0 (see Fig. 6.1). At the points where such a change takes place, secondary bifurcations may occur or the stability of mirror-reflecting or standing waves may change. Future work will focus on extending our techniques to the stability of the latter waves [12] to determine what change in pattern occurs in the system when the phase-locked solutions lose stability and on a more in depth study of the bifurcation interaction points [7].

To close we note that our theoretical predictions could be verified experimentally. Marcus and Westervelt [33] constructed an electric circuit neural network where each element consists of a resistor and capacitor and the elements are connected with nonlinear, delayed amplifiers. They show that this circuit can be quite accurately represented by the model

$$C\dot{u}_i(t) = -\frac{u_i}{R} + \sum_{j=1}^{n} T_{ij} \tanh(Bu_i(t-\tau)), \quad i = 1, \ldots n,$$

by comparing results from linear stability analysis and numerical simulations with those from experiments [32–34]. In particular, their experimental circuits had the following parameter values: $C = 10$ nF, $R = 100$ kΩ, $T_{ij} = T_{ji} \in [-\frac{1}{R}, \frac{1}{R}]$, $T_{ii} = 0$, $n = 2, \ldots, 8$, delays in the range $[0.4, 8]$ RC [33] and gains on the amplifier in the range $[3, 20]$ [34, Fig. 3]. Although the nonlinearity is slightly different, the linear analysis of this model with $T_{ij} = T$ and time rescaled via $t \to \frac{1}{RC}t$ will be the same as that for our model (1.2) with $\alpha = 0$ and $\beta = RTB$. Thus the range of delay and gain values achievable in the experimental system does cover a large portion of the range of values included in Figs. 3.1 and 3.2. Assuming that a self connection with a nonlinear, delayed amplifier could be added to each "neuron" in the circuit, then it should be possible to observe the phenomena we have described above in this experimental system.

Acknowledgements

SAC and JW acknowledge partial financial support in the form of Individual Operating Grants from the Natural Sciences and Engineering Research Council (NSERC) of Canada, and partial financial support from the Mathematics of Information Technology and Complex Systems (MITACS) programme. JW acknowledges partial financial support from the Canada Research Chairs (CRC) programme. The research of IN was supported, in the form of Postdoctoral Fellowships, by the grants to SAC and JW listed above. We thank the reviewers for bringing several important references to our attention.

Appendix

The complicated expressions on the right hand sides of Eqs. (6.12) and (6.19) are given, respectively, by:

$$
\begin{aligned}
H_j[\mathbf{T}_j, \tilde{\mathbf{r}}_j] \stackrel{def}{=}\ & \alpha \mathrm{e}^{-\eta\omega\tau_s}\left\{b\frac{\mathrm{d}T_j}{\mathrm{d}s}(s-\omega\tau_s)+\tilde{r}_j(s-\omega\tau_s)\right\}\\
&+\beta \mathrm{e}^{-\eta\omega\tau}\left\{b\frac{\mathrm{d}T_{j-1}}{\mathrm{d}s}(s-\omega\tau)+\tilde{r}_{j-1}(s-\omega\tau)\right\}\\
&+\beta \mathrm{e}^{-\eta\omega\tau}\left\{b\frac{\mathrm{d}T_{j+1}}{\mathrm{d}s}(s-\omega\tau)+\tilde{r}_{j+1}(s-\omega\tau)\right\}\\
&-\epsilon^2\Bigg[\alpha T_j^2(s-\omega\tau_s)\mathrm{e}^{-\eta\omega\tau_s}\\
&\times\left\{b\frac{\mathrm{d}T_j}{\mathrm{d}s}(s-\omega\tau_s)+\tilde{r}_j(s-\omega\tau_s)\right\}\\
&+\beta T_{j-1}^2(s-\omega\tau)\mathrm{e}^{-\eta\omega\tau}\\
&\times\left\{b\frac{\mathrm{d}T_{j-1}}{\mathrm{d}s}(s-\omega\tau)+\tilde{r}_{j-1}(s-\omega\tau)\right\}\\
&+\beta T_{j+1}^2(s-\omega\tau)\mathrm{e}^{-\eta\omega\tau}\\
&\times\left\{b\frac{\mathrm{d}T_{j+1}}{\mathrm{d}s}(s-\omega\tau)+\tilde{r}_{j+1}(s-\omega\tau)\right\}\Bigg]\\
&-b\left\{\alpha\frac{\mathrm{d}T_j}{\mathrm{d}s}(s-\omega\tau_s)+\beta\frac{\mathrm{d}T_{j-1}}{\mathrm{d}s}(s-\omega\tau)\right.\\
&\left.+\beta\frac{\mathrm{d}T_{j+1}}{\mathrm{d}s}(s-\omega\tau)\right\}\\
&+\epsilon^2 b\left\{\alpha T_j^2(s-\omega\tau_s)\frac{\mathrm{d}T_j}{\mathrm{d}s}(s-\omega\tau_s)\right.\\
&+\beta T_{j-1}^2(s-\omega\tau)\frac{\mathrm{d}T_{j-1}}{\mathrm{d}s}(s-\omega\tau)\\
&\left.+\beta T_{j+1}^2(s-\omega\tau)\frac{\mathrm{d}T_{j+1}}{\mathrm{d}s}(s-\omega\tau)\right\}+\cdots,
\end{aligned}
$$

and

$$
\begin{aligned}
M_j[\mathbf{r}_0, \mathbf{x}_0, \mathbf{x}_1] \stackrel{def}{=}\ & -[b_0\eta_2\omega_0\dot{x}_{j0}(s)+\omega_0\eta_2 r_{j0}(s)+\omega_2\dot{r}_{j0}(s)]\\
&+\alpha[-b_0\ddot{x}_{j0}(s-\omega_0\tau_s)\omega_2\\
&+b_1\dot{x}_{j1}(s-\omega_0\tau_s)+b_2\dot{x}_{j0}(s-\omega_0\tau_s)\\
&-\omega_2\dot{r}_{j0}(s-\omega_0\tau_s)-\tau_s\eta_2\omega_0\{r_{j0}(s-\omega_0\tau_s)\\
&+b_0\dot{x}_{j0}(s-\omega_0\tau_s)\}]\\
&+\beta[-b_0\ddot{x}_{j-1\,0}(s-\omega_0\tau_0)(\omega_0\tau_2+\omega_2\tau_0)\\
&+b_1\dot{x}_{j-1\,1}(s-\omega_0\tau_0)\\
&+b_2\dot{x}_{j-1\,0}(s-\omega_0\tau_0)-(\omega_0\tau_2+\omega_2\tau_0)\\
&\times\dot{r}_{j-1\,0}(s-\omega_0\tau_0)\\
&-\eta_2\omega_0\tau_0\{b_0\dot{x}_{j-1\,0}(s-\omega_0\tau_0)\\
&+r_{j-1\,0}(s-\omega_0\tau_0)\}]\\
&+\beta[-b_0\ddot{x}_{j+1\,0}(s-\omega_0\tau_0)(\omega_0\tau_2+\omega_2\tau_0)\\
&+b_1\dot{x}_{j+1\,1}(s-\omega_0\tau_0)\\
&+b_2\dot{x}_{j+1\,0}(s-\omega_0\tau_0)-(\omega_0\tau_2+\omega_2\tau_0)\\
&\times\dot{r}_{j+1\,0}(s-\omega_0\tau_0)\\
&-\eta_2\omega_0\tau_0\{b_0\dot{x}_{j+1\,0}(s-\omega_0\tau_0)\\
&+r_{j+1\,0}(s-\omega_0\tau_0)\}]\\
&-\alpha x_{j0}^2(s-\omega_0\tau_s)[b_0\dot{x}_{j0}(s-\omega_0\tau_s)\\
&+r_{j0}(s-\omega_0\tau_s)]\\
&-\beta[b_0x_{j-1\,0}^2(s-\omega_0\tau_0)\dot{x}_{j-1\,0}(s-\omega_0\tau_0)\\
&+r_{j-1\,0}(s-\omega_0\tau_0)]\\
&-\beta[b_0x_{j+1\,0}^2(s-\omega_0\tau_0)\dot{x}_{j+1\,0}(s-\omega_0\tau_0)\\
&+r_{j+1\,0}(s-\omega_0\tau_0)]\\
&-b_0[-\alpha\omega_2\ddot{x}_{j0}(s-\omega_0\tau_s)\\
&-\beta(\omega_0\tau_2+\omega_2\tau_0)\ddot{x}_{j-1\,0}(s-\omega_0\tau_0)\\
&-\beta(\omega_0\tau_2+\omega_2\tau_0)\ddot{x}_{j+1\,0}(s-\omega_0\tau_0)]\\
&-b_1[\alpha\dot{x}_{j1}(s-\omega_0\tau_s)+\beta\dot{x}_{j-1\,1}(s-\omega_0\tau_0)\\
&+\beta\dot{x}_{j+1\,1}(s-\omega_0\tau_0)]\\
&-b_2[\alpha\dot{x}_{j0}(s-\omega_0\tau_s)+\beta\dot{x}_{j-1\,0}(s-\omega_0\tau_0)\\
&+\beta\dot{x}_{j+1\,0}(s-\omega_0\tau_0)]\\
&+b_0[\alpha x_{j0}^2(s-\omega_0\tau_s)\dot{x}_{j0}(s-\omega_0\tau_s)\\
&+\beta x_{j-1\,0}^2(s-\omega_0\tau_0)\dot{x}_{j-1\,0}(s-\omega_0\tau_0)\\
&+\beta x_{j+1\,0}^2(s-\omega_0\tau_0)\dot{x}_{j+1\,0}(s-\omega_0\tau_0)].
\end{aligned}
$$

References

[1] I. Barbălat, Systèmes d'équations differentielles d'oscillations non linéaires, Rev. Math. Pures Appl. 4 (1959) 267–270.

[2] J. Bélair, Stability in delayed neural networks, in: J. Wiener, J. Hale (Eds.), Ordinary and Delay Differential Equations, Longman Scientific and Technical, New York, 1992, pp. 6–9.

[3] J. Bélair, Stability in a model of a delayed neural network, J. Dyn. Syst. Differential Equations 5 (1993) 607–623.

[4] J. Bélair, S.A. Campbell, Stability and bifurcations of equilibria in a multiple delayed differential equation, SIAM J. Appl. Math. 54 (1994) 1402–1423.

[5] J. Bélair, S.A. Campbell, P. van den Driessche, Frustration, stability and delay-induced oscillations in a neural network model, SIAM J. Appl. Math. 46 (1996) 245–255.

[6] J. Bélair, S. Dufour, Stability in a three-dimensional system of delay-differential equations, Canad. Appl. Math. Quart. 4 (1996) 136–156.

[7] S. Bungay, S.A. Campbell, Y. Yuan, Bifurcation interactions in a ring of identical cells with delayed coupling, Preprint, 2006.

[8] S.A. Campbell, Stability and bifurcation of a simple neural network with multiple time delays, Fields Inst. Commun. 21 (1999) 65–79.

[9] S.A. Campbell, J. Bélair, T. Ohira, J. Milton, Limit cycles, tori, and complex dynamics in a second-order differential equations with delayed negative feedback, J. Dynam. Differential Equations 7 (1) (1995) 213–236.

[10] S.A. Campbell, J. Bélair, T. Ohira, J. Milton, Complex dynamics and multistability in a damped harmonic oscillator with delayed negative feedback, Chaos 5 (4) (1995) 640–645.

[11] S.A. Campbell, S. Ruan, J. Wei, Qualitative analysis of a neural network mode with multiple time delays, Internat. J. Bifur. Chaos 9 (8) (1999) 1585–1595.

[12] S.A. Campbell, Y. Yuan, S. Bungay, Equivariant Hopf bifurcation in a ring of identical cells with delayed coupling, Nonlinearity 18 (2005) 2827–2846.

[13] Y. Chen, J. Wu, Existence and attraction of a phase-locked oscillation in a delayed network of two neurons, Differential Integral Equations 14 (2001) 1181–1236.

[14] Y. Chen, J. Wu, Slowly oscillating periodic solutions for a delayed frustrated network of two neurons, J. Math. Anal. Appl. 259 (2001) 188–208.

[15] Y. Chen, J. Wu, The asymptotic shapes of periodic solutions of a singular delay differential system, in: Celebration of Jack K. Hale's 70th Birthday, Part 4 (Atlanta, GA/Lisbon, 1998), J. Differential Equations 169 (2001) 614–632 (special issue).
[16] Y. Chen, J. Wu, Minimal instability and unstable set of a phase-locked periodic orbit in a delayed neural network, Physica D 134 (1999) 185–199.
[17] Y. Chen, J. Wu, T. Krisztin, Connecting orbits from synchronous periodic solutions in phase-locked periodic solutions in a delay differential system, J. Differential Equations 163 (2000) 130–173.
[18] T. Faria, L.T. Magalhães, Normal forms for retarded functional differential equations with parameters and applications to Hopf bifurcations, J. Differential Equations 122 (1995) 181–200.
[19] M. Golubitsky, I. Stewart, D.G. Schaeffer, Singularities and Groups in Bifurcation Theory, Springer-Verlag, New York, 1988.
[20] K. Gopalsamy, Stability and Oscillations in Delay Differential Equations of Population Dynamics, Kluwer Academic Publishers, The Netherlands, 1992.
[21] K. Gopalsamy, I. Leung, Delay induced periodicity in a neural netlet of excitation and inhibition, Physica D 89 (1996) 395–426.
[22] J. Guckenheimer, P. Holmes, Nonlinear Oscillations, Dynamical Systems, and Bifurcations of Vector Fields, Springer-Verlag, New York, 1983.
[23] J. Haddock, J. Terjeki, Liapunov–Razumikhin functions and an invariance principle for functional differential equations, J. Differential Equations 48 (1983) 95–122.
[24] A. Halanay, Differential Equations, in: Mathematics in Science and Engineering, vol. 23, Academic Press, New York, 1966.
[25] J. Hale, Theory of Functional Differential Equations, Springer-Verlag, New York, 1977.
[26] J. Hale, W. Huang, Global geometry of the stable regions for two delay differential equations, J. Math. Anal. Appl. 178 (1993) 344–362.
[27] J. Hale, S.M.V. Lunel, Introduction to Functional Differential Equations, Springer-Verlag, New York, 1993.
[28] L. Huang, J. Wu, Nonlinear waves in networks of neurons with delayed feedback: pattern formation and continuation, SIAM J. Math. Anal. 34 (4) (2003) 836–860.
[29] V.B. Kolmanovskii, V.R. Nosov, Stability of functional differential equations, in: Mathematics in Science and Engineering, vol. 180, Academic Press, 1986.
[30] W. Krawcewicz, J. Wu, Theory and applications of Hopf bifurcations in symmetric functional-differential equations, Nonlinear Anal. 35 (1999) 845–870.
[31] J.M. Mahaffy, P.J. Zak, K.M. Joiner, A geometric analysis of stability regions for a linear differential equation with two delays, Internat. J. Bifur. Chaos 5 (1995) 779–796.
[32] C.M. Marcus, F.R. Waugh, R.M. Westervelt, Nonlinear dynamics and stability of analog neural networks, Physica D 51 (1991) 234–247.
[33] C.M. Marcus, R.M. Westervelt, Basins of Attraction for Electronic Neural Networks, in: D.S. Anderson (Ed.), Neural Information Processing Systems, Denver, CO, 1987, AIP, 1988, pp. 524–533.
[34] C.M. Marcus, R.M. Westervelt, Stability of analog neural networks with delay, Phys. Rev. A 39 (1989) 347–359.
[35] J. Milton, Dynamics of small neural populations, in: CRM Monograph Series, vol. 7, American Mathematical Society, Providence, RI, 1996.
[36] I. Ncube, S.A. Campbell, J. Wu, Change in criticality of synchronous Hopf bifurcation in a multiple-delayed neural system, Fields Inst. Commun. 36 (2003) 179–194.
[37] R. Nussbaum, Differential delay equations with two time delays, Mem. Amer. Math. Soc. 16 (1978).
[38] L. Olien, J. Bélair, Bifurcations, stability and monotonicity properties of a delayed neural network, Physica D 102 (1997) 349–363.
[39] G. Orosz, G. Stépán, Hopf bifurcation calculations in delayed systems with translational symmetry, J. Nonlinear Sci. 14 (6) (2004) 505–528.
[40] G. Orosz, R.E. Wilson, B. Krauskopf, Global bifurcation investigation of an optimal velocity traffic model with driver reaction time, Phys. Rev. E 70 (2) (2004) 026207.
[41] K. Pakdaman, C.P. Malta, C. Grotta-Ragazzo, J.-F. Vibert, Delay-induced transient oscillations in a two-neuron network, Resenhas (1997) 45–54.
[42] K. Pakdaman, C.P. Malta, C. Grotta-Ragazzo, J.-F. Vibert, Effect of delay on the boundary of the basin of attraction in a self-excited single neuron, Neural Comput. 9 (1997) 319–336.
[43] K. Pakdaman, C.P. Malta, C. Grotta-Ragazzo, O. Arino, J.-F. Vibert, Transient oscillations in continuous-time excitatory ring neural networks with delay, Phys. Rev. E 55 (1997) 3234–3248.
[44] K. Pakdaman, C. Grotta-Ragazzo, C.P. Malta, Transient regime duration in continuous-time neural networks with delay, Phys. Rev. E 58 (1998) 3623–3627.
[45] K. Pakdaman, C. Grotta-Ragazzo, C.P. Malta, O. Arino, J.-F. Vibert, Effect of delay on the boundary of the basin of attraction in a system of two neurons, Neural Netw. 11 (1998) 509–519.
[46] D.H. Sattinger, Topics in Stability and Bifurcation Theory, in: Lecture Notes in Mathematics, vol. 309, Springer, Berlin, 1973.
[47] L.P. Shayer, S.A. Campbell, Stability, bifurcation and multistability in a system of two coupled neurons with multiple time delays, SIAM J. Appl. Math. 61 (2) (2000) 673–700.
[48] G. Stépán, Retarded Dynamical Systems, in: Pitman Research Notes in Mathematics, vol. 210, Longman Group, Essex, 1989.
[49] G. Stépán, G. Haller, Quasiperiodic oscillations in robot dynamics, Nonlinear Dynam. 8 (1995) 513–528.
[50] J. Wei, S. Ruan, Stability and bifurcation in a neural network model with two delays, Physica D 130 (1999) 255–272.
[51] J. Wu, Symmetric functional differential equations and neural networks with memory, Trans. Amer. Math. Soc. 350 (1998) 4799–4838.
[52] J. Wu, Introduction to Neural Dynamics and Signal Transmission Delay, De-Gruyter, Berlin, 2001.
[53] J. Wu, T. Faria, Y.S. Huang, Synchronization and stable phase-locking in a network of neurons with memory, Math. Comput. Modelling 30 (1999) 117–138.